

---

# Geodynamics and Volcanism in the Kos-Yali-Nisyros Volcanic Field

# 2

Paraskevi Nomikou, Dimitrios Papanikolaou  
and Volker Jörg Dietrich

---

## Abstract

This chapter encompasses a short review on the general aspects of the geodynamics in the southeast Aegean region, in the context of the plate convergence between the African plate and the Anatolian and Aegean microplates. Southeast-ward subduction of oceanic lithosphere and crust of a remnant Thethys ocean beneath the microplates are responsible for the generation of magmatism and volcanism during the past 5 million years. This formed the South Aegean Volcanic Arc and in particular the Kos-Yali-Nisyros-Tilos volcanic field in the southeast corner. The chapter mostly deals with the description of morphotectonic structures, obtained from a combination of onshore and offshore data, generated during numerous cruises since the European GEOWARN project seventeen years ago. The cruises focussed on a precise bathymetric exploration to determine the seafloor morphology with its young sedimentary cover, submarine volcanic features and fault zones within the different basins,

---

**Electronic supplementary material** The online version of this chapter (doi:[10.1007/978-3-319-55460-0\\_2](https://doi.org/10.1007/978-3-319-55460-0_2)) contains supplementary material, which is available to authorized users.

---

P. Nomikou · D. Papanikolaou  
Faculty of Geology and Geoenvironment,  
National & Kapodistrian University of Athens,  
157 84 Athens, Greece  
e-mail: [evinom@geol.uoa.gr](mailto:evinom@geol.uoa.gr)

D. Papanikolaou  
e-mail: [dpapan@geol.uoa.gr](mailto:dpapan@geol.uoa.gr)

V.J. Dietrich (✉)  
Institute of Geochemistry and Petrology,  
Swiss Federal Institute of Technology, ETH Zurich,  
ETH-Zentrum, 8092 Zürich, Switzerland  
e-mail: [volker.dietrich@erdw.ethz.ch](mailto:volker.dietrich@erdw.ethz.ch)

troughs and horsts. Geological outlines and maps are given for all volcanic eruptive centers: Kos Island and the distribution of the 161,000 years old Kos Plateau Tuff, Nisyros Volcano, Yali Island, Strongyli Volcano, Avyssos submarine crater, the volcanic islet Pergousa and Pachia and the Kondelioussa islet.

## 2.1 Introduction: Aegean Magmatism and Volcanism as Result of Cenozoic Plate Motions

The Kos-Yali-Nisyros Volcanic Field (Fig. 2.1) comprises the eastern sector of the South Aegean Volcanic Arc (SAVA). The arc is regarded as a magmatic expression of the ongoing

north-eastward-directed subduction of the African plate beneath the Aegean-Anatolian microplate, which started around 5 Ma at the beginning of Pliocene (McKenzie 1972; Le Pichon and Angelier 1979; Papanikolaou 1993; Jackson 1993, 1994). All volcanic centers are located above a  $38^\circ$  dipping Benioff zone in the depth range of 130–150 km (Makropoulos and Burton 1984).

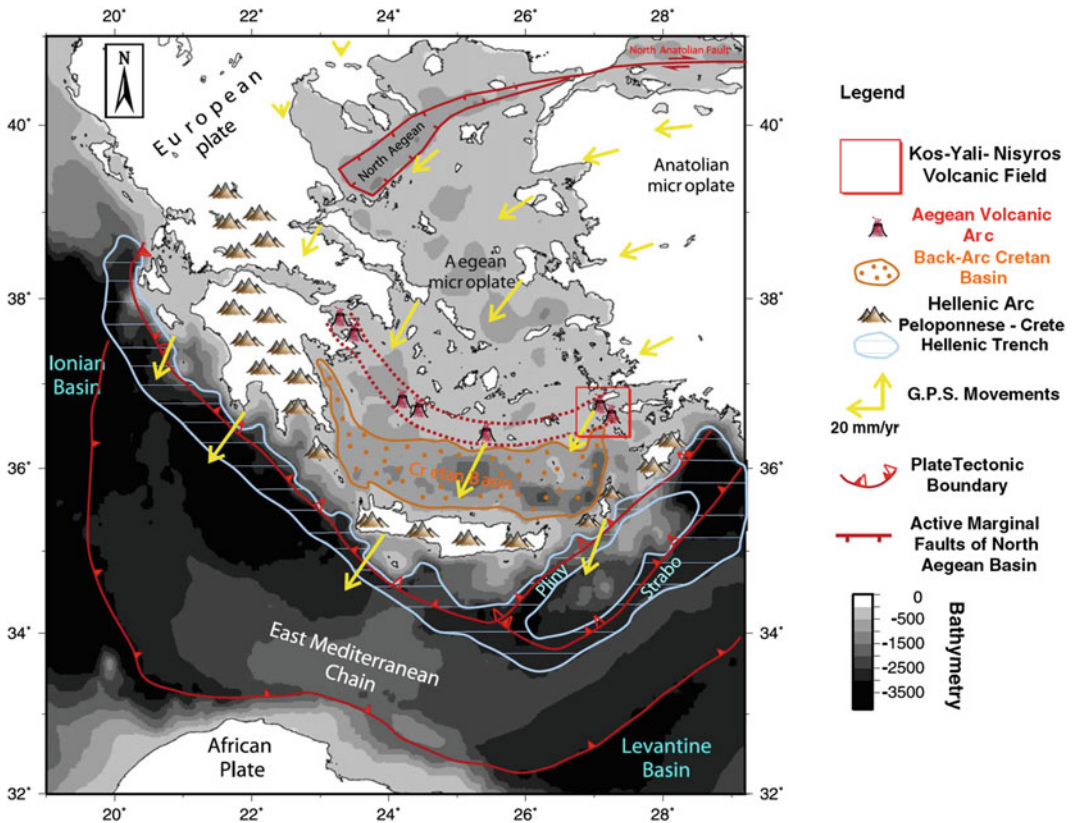


**Fig. 2.1** Simplified map of the present day geodynamic structure of the Hellenic arc, showing the modern South Aegean Volcanic Arc developed behind the Hellenic trench, the Peloponnese-Crete island arc and the Cretan back-arc basin after Nomikou and Papanikolaou (2010b;

Nomikou et al. 2013a). Note that the African plate to the south is subducting beneath the Eurasian plate to the north along the red lines just to the south of Crete. Yellow arrows indicate relative motions of approximately 35 mm/year of the Aegean-Anatolian microplate towards the African plate

The early continent/continent collision of the Aegean-Anatolian microplate (South Aegean, Menderes, Bey Daglan) began during Middle to Late Eocene and continuing into Lower Oligocene (Robertson and Dixon 1984; Collins et al. 1998). Synchronous anticlockwise rotational (northeast- to northward directed) movement of the Adriatic-Apulian promontory led to its subduction beneath the Aegean-Anatolian microplate. Continuation into Early Miocene caused compression and crustal thickening in the Hellenides, as well as extension in the external realm in northern Greece. As result of subduction and extension, magmatic activity occurred throughout the extensional realm from Middle Eocene to Late Miocene (Innocenti et al. 1981; Fytikas et al. 1984; Pe-Piper et al. 1994; for extensive review see Pe-Piper and Piper 2002).

Subduction of the south-eastern Mediterranean oceanic crust synchronously coupled with extensional magmatism during Miocene in the central and south-eastern Aegean, manifested by numerous granitic intrusions and adjacent volcanics in several Cycladic and Dodecanese islands and in the Bodrum peninsula (Anatolian coast). At about 5 Ma the spatial distribution of magmatism and volcanism shifted southward and westward and led to the development of the South Aegean volcanic arc. At this time the “consolidation” of the central Aegean block took place due to lithospheric strike-slip movements, which are expressed by the propagation of the “North Anatolian Fault” reaching the northeastern Aegean realm. South-westward motion of the Aegean block with up to 35 mm/year (Jackson 1994) and westward motion of the Anatolian block with about 20 mm/year accompanied by vertical displacements initiated strong lithospheric deformation (Fig. 2.1). The differential convergence rates between the north-eastward directed subduction of oceanic crust and African plate relative to the different blocks of the Eurasian lithosphere may have caused rapid extension, thinning of the continental Aegean back-arc region and thus, induced an adiabatic upwelling mantle.

## 2.2 The South Aegean Volcanic Arc

The volcanic islands of the South Aegean Sea, Aegina, Methana, Poros, Milos, Santorini, Kolombo, Yali Nisyros, and Kos define a volcanic island arc, which extends over a distance of approximately 600 km from Corinth in the Saronic Gulf bordering Attica and the Peloponnese to the islands of Kos and Nisyros near the Turkish coast (Fig. 2.1). In general, the volcanic rocks of the South Aegean volcanic arc belong to the calc-alkaline and high-K calc-alkaline (mainly of Pliocene age) series. Tholeiitic basalts occur in the Santorini islands.

Two different magmato-volcanic environments can be distinguished within the South Aegean volcanic arc, differing in age, magma types, volumes, volcanic edifices, and spatial distribution. The volcanic centers seem to be aligned by large fracture zones, trending E–W to NW–SE for the western part including Susaki, Poros, Methana, and Aegina (Dietrich et al. 1991; Hurni et al. 1995) and mainly NE–SW for the central and eastern parts of the arc including Milos, Santorini, Yali, Kos and Nisyros (Francalanci et al. 2005; Pe-Piper and Piper 2005). The volcanic activity started around 4.7 Ma and continued until present with the active but dormant volcanoes Methana, Santorini, Kolombo, and Nisyros. The western volcanic centers developed mainly as monogenic structures along fissures, plugs and domes whereas in the central and eastern volcanic islands composite volcanoes with caldera structures were formed.

The eastern sector of the island arc, including the islands of Kos, Yali and Nisyros, seems to be geodynamically very active, since it comprises the largest volumes of volcanic products, which were emitted during the past 161,000 years and is at present a tectonically active region (McKenzie, 1972; Drakopoulos and Delibasis 1982; LePichon 1982; Fytikas et al. 1984; Jackson 1994; Smith et al. 1996).

The magmatic processes started in Late Miocene and continued throughout 15 million years leading to the present day situation on the island

of Nisyros (Burri et al. 1967; Pe and Piper 1972; Fytikas et al. 1976, 1984; Innocenti et al. 1981; Pe-Piper and Piper 2002). In this respect, all volcanic and plutonic phases in the eastern Aegean islands from Mytilini through Chios, Samos, Izmir, Furni, Patmos, Bodrum and Kos down to Nisyros can be explained. The largest eruption, however occurred 161,000 years ago, which led to the largest eruption in the Eastern Mediterranean emitting more than  $100 \text{ km}^3$  of pyroclastic material, the Kos Plateau tuff, which devastated an area of more than  $3000 \text{ km}^2$  (Keller 1969; Stadlbauer 1988; Keller et al. 1990; Allen and Cas 1998a). Deposits occur on Kalymnos, on the peninsula of Datça and Tilos. The center of this catastrophic eruption was probably located north to northeast of Yali. Several hundreds of cubic kilometres of magmas were emplaced along the NE striking Kos-Tilos horst-graben system from the upper mantle into low crustal levels.

As the result of such a voluminous magma deficit in the underground a caldera of a diameter of 15–20 km must have been formed (Fig. 2.2), now covered with volcano-sedimentary products from younger eruptions and debris with an

average thickness of 10 km. During the time span of 161,000 years the volcanic edifices of Nisyros, Yali, Pergousa, Pachia and Strongyli have grown in its inferred central part.

Nisyros and the surrounding islets have been formed during the Late Pleistocene-Holocene within an ENE-WSW trending neotectonic graben. The island of Nisyros is mainly composed of Quaternary calc-alkaline volcanic rocks which are represented by alternating lava flows, pyroclastic layers and viscous lava domes, formed during several cycles from 160 to 25 ka. The dominant feature on the island is a truncated cone with a base diameter of 8 km and a central caldera of 4 km in diameter (Di Paola 1974; Papanikolaou et al. 1991; Volentik et al. 2005). The Yali and Strongyli volcanic islands, located north of Nisyros, along with the submarine volcano of Avyssos, are prominent features in the area, bounded by NE-SW normal faults (Wagner et al. 1976; Allen and Cas 2001; Nomikou and Papanikolaou 2010a).

Figure 2.2 shows a magmato-tectonic model to demonstrate the close relationship between magmatism/volcanism, seismicity and structural

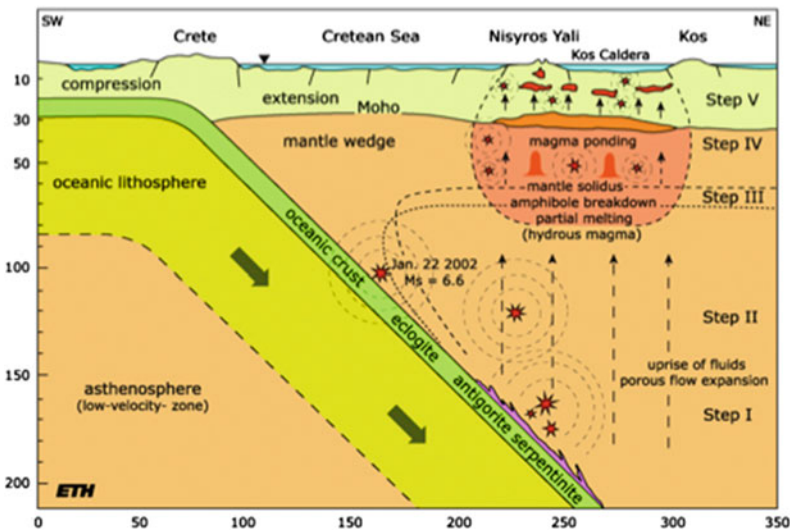


**Fig. 2.2** The Magmato-Tectonic model of the eastern sector of the Aegean volcanic arc in a SW-NE cross-section from Crete to Kos. Depth and position of the subduction zone is inferred from the spatial distribution of deep earthquakes (Drakopoulos and Delimbasis

1982; Makropoulos and Burton 1984; Makropoulos et al. 1989). The encircled area marks the agglomeration of seismic activity in the Kos-Yali-Nisyros volcanic field. Source GEOWARN (2003)

configuration in the eastern sector of the Aegean volcanic arc. The increase of geodynamic activity can only be understood if the processes of magma generation, emplacement, fluid behaviour and tectonic environment are known. Magma generation and emplacement have been subdivided into five steps and linked to seismic activity and crustal deformation. For this reason, the volcanic islands of Milos, Santorini, Kos and Nisyros are dominated by large composite volcanoes with summit calderas and hydrothermal systems. Pyroclastic rocks of rhyodacitic to rhyolitic composition are predominant. This is an expression of the existence of relatively large, shallow crustal magma chambers allowing further crystal fractionation and crustal contamination, finally leading to highly explosive activity and Plinian eruptions.

The base of the central and eastern volcanic arc rests on normal and partially thinned continental crust (Makris 1977) and underwent several stages of deformation and metamorphism during the Alpine orogeny from Cretaceous to late Tertiary (Smith 1971). Thus, structural configuration of the continental crust can be regarded as a pile of nappes of the Hellenides, part of the “Alpine Orogen”. The islands of Milos, Santorini and Nisyros show today a pronounced extensional lithospheric stress field, which favours upwelling of the asthenosphere, partial melting of peridotitic mantle rocks, uprise of primitive basaltic melts through a 25–30 km thick crust and the generation of shallow magma chambers.

### 2.3 The Kos-Yali-Nisyros-Volcanic Field

The Kos-Yali-Nisyros Volcanic Field (Figs. 2.1 and 2.3) covers the most complex eastern part of the Alpine-Hellenide orogen, which structurally merges into the nappe pile of the Taurides of SW Turkey. Since Late Miocene the entire area has been dissected by major tectonic lineaments such as “Horst-Graben systems” bordered by NE-SW and WNW-ESE faults, along which uplift, down-faulting and strike-slip movements occurred.

Normal faulting occurred along a NW-SE (at Miocene time probably N-S) lineament which extended in the Dodecanese Islands from Chios through Furni, the west of Patmos southeastward into the island of Rhodes and led to formation of the Antimachia graben. Extensional movements, directed towards SW, downdropped basement blocks along listric faults. Strong uplift and erosion of the “Menderes metamorphic complex” the “Cine sub-massif” and the “Bey Daglari unit” generated several E-W trending Neogene basins (e.g. “horst-graben” systems from North to South): Gediz graben, Küçük Menderes graben, the Büyük Menderes graben, and the Kerme Körfezi graben, the eastern extension of the East Kos Basin. The eastern boundary of the Hellenic arc is defined by the sinistral Rhodes Transform Fault, implying a dominant extension regime Lower Miocene (Müller and Kahle 1993).

Synchronously, calc-alkaline magmas derived by partial melting of sub-continental mantle above down-going Cenozoic oceanic lithosphere segregated and accumulated beneath the collided Hellenic nappe piles and Lycian Taurides thrust sheets at the mantle/crust boundary.

The intersection of the N-S (at present NW-SE) and E-W “horst-graben” systems in the eastern Aegean Sea led to pronounced centers of weakness in the stress pattern of the rigid crust. Changes of the crustal stress field due to extensional, rotational and strike-slip movements at different crustal levels (“stockwerks” of nappe piles) favoured the migration of the deep magmas to upper crustal levels.

These processes started in Late Miocene and continued throughout 15 million years leading to the present day situation on the island of Nisyros (Burri et al. 1967; Pe and Piper 1972; Fytikas et al. 1976, 1984; Innocenti et al. 1981; Pe-Piper and Piper 2002). In this respect, all volcanic and plutonic phases in the eastern Aegean islands from Mytilini through Chios, Samos, Izmir, Furni, Patmos, Bodrum and Kos down to Nisyros can be explained. At present the Kos-Yali-Nisyros-Tilos volcanic field still is a region of high tectonic unrest (Drakopoulos and Delibasis 1982; Jarigge 1978; Makropoulos and Burton 1984; Papadopoulos 1984; Papadopoulos et al. 1986; Smith et al. 1996).



### 2.3.1 Morphotectonic Structures, a Combination of Onshore/Offshore Data

The neotectonic (post Plio- and Pleistocene) structures of the Kos-Yali-Nisyros volcanic field are demonstrated by the outcrops of the “Alpine basement”. These pre-Miocene sedimentary and intrusive rocks are found in uplifted blocks—neotectonic horsts separated by the recent and actual marine basins where subsidence has prevailed during the last few millions of years. The Alpine basement in the submarine area occurs at

great depths below the sea floor covered by thick post-Alpine sediments.

Thus, the submarine area between Kos and Tilos islands constitutes a regional neotectonic horst-graben system, which extends from the Datça peninsula in the coastal area of Minor Asia towards SW (Figs. 2.3 and 2.4). In addition, an intermediate Kondelioussa horst exists dividing the basins on both sides of Nisyros. Nisyros and surrounding islets represent the volcanic structures that have intruded within this regional graben as was confirmed by geothermal drillings (Geotermica Italiana 1983, 1984), which

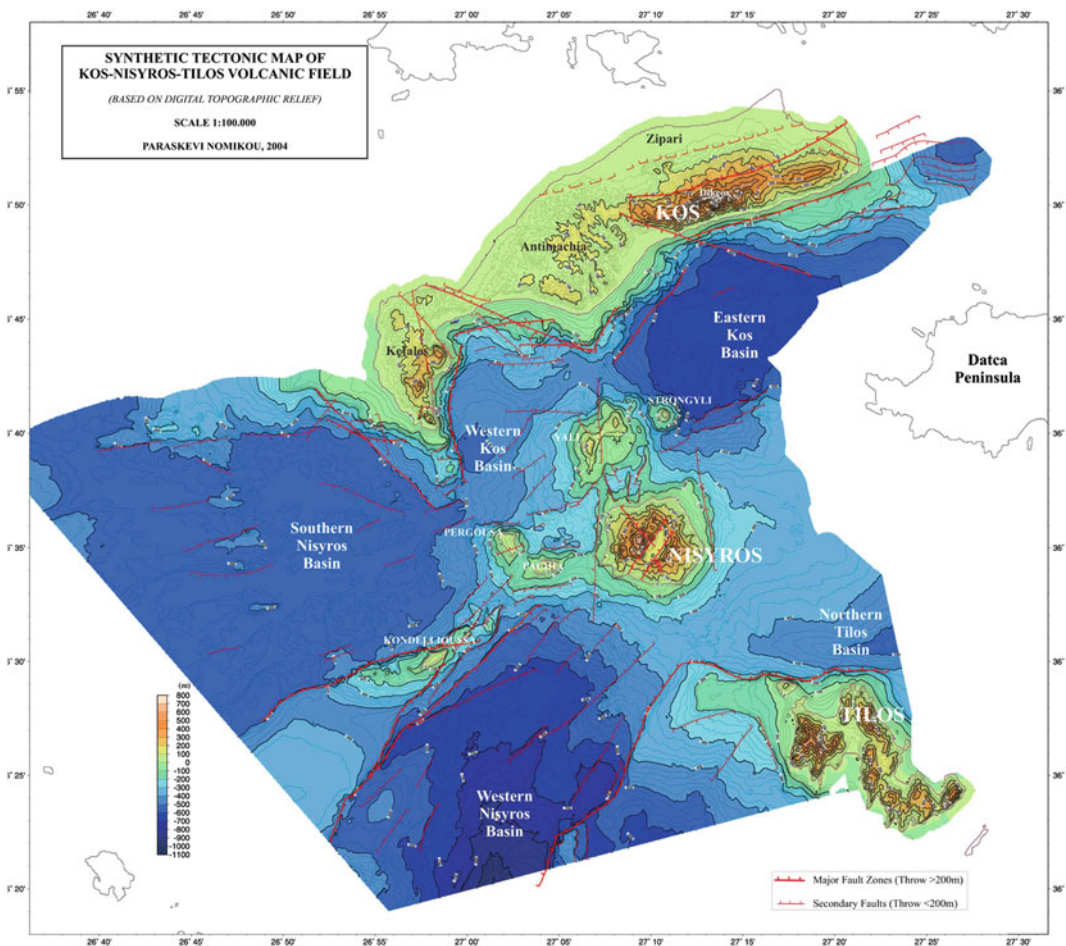


**Fig. 2.3** Synthetic tectonic map of Kos-Yali-Nisyros volcanic field based on data obtained from multi-beam bathymetric surveys and combined with onshore hypsometric data (Electronic Supplementary Material Appendix). 1 Eastern Kos Basin, 2 Western Kos Basin,

3 Western Nisyros Basin, 4 Southern Nisyros Basin, 5 Tilos Basin, 6 Pachia-Pergousa Basin, 7 Yali-Nisyros Basin. *Source* Nomikou (2004), Nomikou et al. (2004), Nomikou and Papanikolaou (2010b)

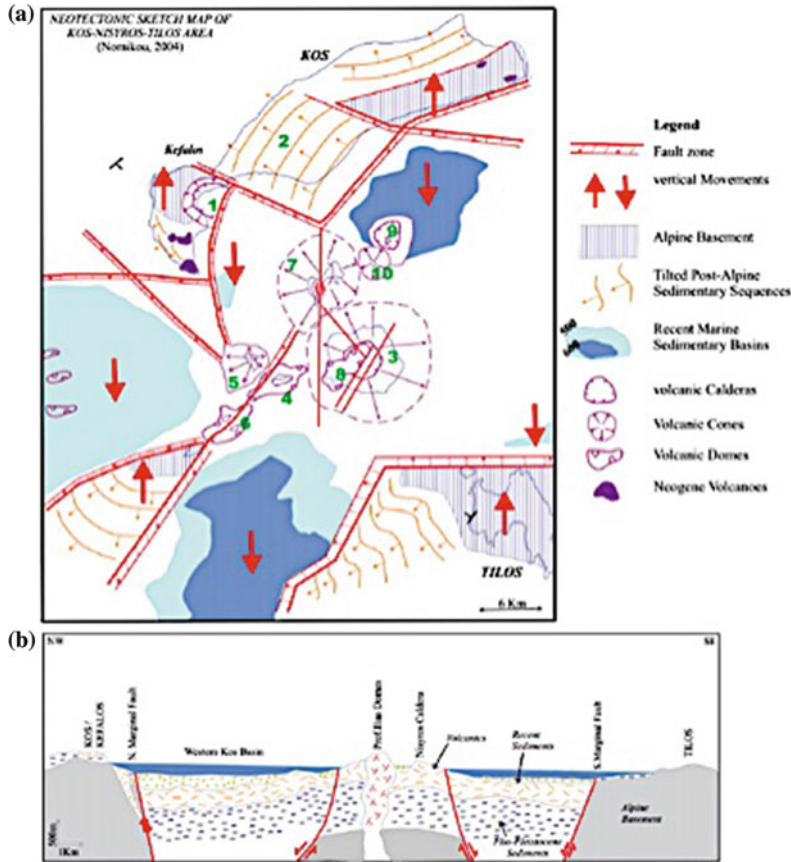


**Fig. 2.4** **a** Interpretative neotectonic sketch map of Kos-Yali-Nisyros-Tilos volcanic field with distinction of the volcanic centers group (modified after Papanikolaou and Nomikou 2001; Nomikou 2004; Nomikou et al. 2013a). 1 Kefalos (500 ka), 2 Kos Plateau Tuff (161 ka) 3–10: late pleistocene-holocene volcanoes, 3 Nisyros stratovolcano, 4 Pachia, 5 Pergousa, 6 East Kondelioussa, 7 Yali, 8 Prophitis Ilias, 9 Avyssos, 10 Strongyli; **b** schematic tectonic profile from Kos/Kefalos Peninsula to Tilos. The intermediate uplift of the Nisyros volcanic area in the form of a minor horst is shown within the neotectonic graben structure

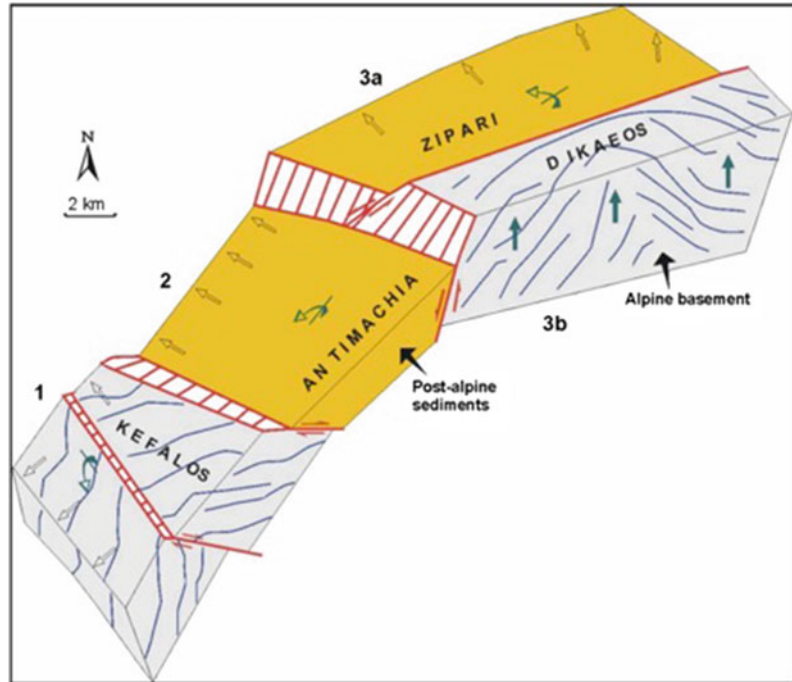
encountered Alpine basement rocks at 1800 m depth.

A morphotectonic map of the area of Kos-Nisyros-Tilos can be transformed to a neotectonic sketch map (Fig. 2.4a, b) characterized by the distinction of neotectonic blocks bordered by major faults. Each neotectonic block is characterised by its morphology, which is different across its tectonic margins from that of the neighbouring blocks. The difference may comprise the intensity of the relief, expressed by the slope gradients and/or the relief orientation, and its average elevation either positive or negative. Additionally, each neotectonic block may present a different tectono-stratigraphy referring to the Alpine

formations and/or the post-Alpine sediments and eventual volcanic formations. The general dip of the strata and of the volcanic products may indicate the nature of vertical and/or tilt motions during or after the deposition of each geological formation.

Kos Island constitutes a synthetic tectonic mega-horst of ENE-WSW direction including three successive multi-blocks: Kefalos multi-block (1) in the west divided in Kefalos Peninsula, Western Kefalos and Southern Kefalos, Antimachia block (2) in the middle and Dikeos multi-block (3) in the east divided in Dikeos Mt. (3a) and Zipari block (3b) (Fig. 2.5). All these blocks constitute the Kos mega-horst bordering from the north the successive

**Fig. 2.5** Neotectonic blocks of Kos: 1 Kefalos, 2 Antimachia, 3a Zipari, 3b Dikeos (Papanikolaou and Nomikou 1998; Nomikou 2004)



grabens/basins of blocks 4, 5 and 6. However, the tectonic horsts showing relative uplift from all surrounding blocks are only blocks 1a of Kefalos peninsula and 3a of Dikeos mountain.

The Antimachia tectonic block (2) in Fig. 2.5 comprises outcrops only of Neogene and Quaternary sediments observed below the widespread Upper Pleistocene volcanic breccia and pumice of the “Kos Plateau Tuff” which forms the planar surface of the Antimachia plateau and is characterized as a tectonic graben between the adjacent tectonic horsts of Kefalos (1) and Dikeos (3b). However, it presents an important uplift relative to the submarine tectonic grabens (Fig. 2.5) of the Western Kos Basin and the Eastern Kos Basin (Fig. 2.3). This relative uplift is confirmed by the occurrence of marine Pleistocene sediments on the Antimachia plateau at altitudes around 100–120 m. The lack of outcrops of Alpine formations and of Miocene continental deposits (known from the adjacent horsts of Kefalos and Dikeos) imply a relative subsidence of more than 1000 m with respect to Dikeos and more than 600 m with respect to Kefalos. The tectonic throw between Antimachia

block and Zipari block is only a few hundred meters. The post-Alpine sedimentary formations below the Kos Plateau Tuff are tilted to the NW by 10–15° around an ENE–WSW axis.

The tectonic block of Zipari (3a) comprises thick alluvial sediments observed all along the northern coast of Kos and Neogene continental sediments tilted towards the north. Small outcrops of Alpine rocks belonging to the Prohitis Ilias/Pindos tectonic unit occur in the hills of Zipari block. Thus, there is strong subsidence in relation to the tectonic horst of Dikeos (3a) and a relative uplift in relation to the tectonic block of Antimachia (2).

The two marginal tectonic blocks of Kefalos are subsided areas of the Kefalos Peninsula horst but they are uplifted blocks in relation to the Western Nisyros Basin. The tectonic block of Kos-Knidus channel also presents subsidence in relation to the tectonic horst of Dikeos (3a) and uplift in relation to the tectonic graben of the Eastern Kos Basin.

The Tilos horst (Fig. 2.4a, b) is made of Mesozoic “Alpine formations” covered by post-Alpine sediments occurring on the submarine plateau developed towards the southwest of Northern Tilos Island. The sediments of this



plateau look very similar in the lithoseismic profiles with those occurring over the neighbouring plateau of Kondelioussa and show the same tilt towards the SW. The tectonic margins of Tilos horst are made by a NE-SW oriented fault towards the Southern Nisyros Basin and another fault of EW direction towards the Northern Tilos Basin. Both faults produce an asymmetry of the basins with the deepest subhorizontal parts reaching the margins of Tilos horst. The fault throw is more than 1 km as the depths of the basins (about 600 m in Northern Tilos and more than 1000 m in Southern Nisyros) and the minimum thickness of the sediments (more than 600 m detected on the airgun profiles) imply.

### 2.3.2 Submarine Volcano-Sedimentary Basins

Five submarine basins (Fig. 2.3) can be distinguished within the regional graben of the Kos-Tilos area. The detailed “swath bathymetric map” permitted the delineation of the following five main marine basins in the circum-volcanic area of Nisyros (Fig. 2.3): (1) Eastern Kos Basin, (2) Western Kos Basin, (3) Western Nisyros Basin, (4) Southern Nisyros Basin and (5) Tilos Basin. Additionally, two smaller basins occur within the shallow-water intra volcanic area of Nisyros: (6) Pachia-Pergousa Basin and (7) Yali-Nisyros Basin. The intermediate horst of Kondelioussa and its northeastward volcanic prolongation of Nisyros and surrounding islets separate three basins (1, 2 and 5) along the northern sub-graben and another two basins (3 and 4) along the southern sub-graben.

#### 2.3.2.1 Eastern Kos Basin

The Eastern Kos Basin (Fig. 2.6), representing a main block of a tectonic graben, is bordered to the north by the steep southern slopes of Dikeos Mountain whereas towards the south it is separated from the Tilos Basin by the rise connecting Nisyros Island with the Datça peninsula. To the

east it continues into the basin developed north of Datça peninsula and south of eastern Kos. To the west it is bordered from the Western Kos Basin by the Yali-Kos rise and to the southwest by the very steep volcanic cone of Strongyli islet, which emerges to 120 m altitude from a depth of 600 m. The general orientation of the basin is ENE-WSW, parallel to the orientation of Kos Island. This orientation is due to a major neotectonic fault running parallel to the coast of Kos for more than 20 km, which has subsided the Eastern Kos Basin with respect to the Dikeos mountain with a throw more than 700 m. A number of submarine canyons have been detected from shallow depths of about 150 m to approximately 500 m where the morphological slopes become very shallow and grade to the sub horizontal basinal part at depths around 650 m. More than 600 m of Neogene sediments have been detected below the sea floor.

The irregular morphology of the southern basinal area is unique in this basin with a possible submarine caldera occurring immediately northeast of the base of the Strongyli volcanic cone (Figs. 2.6, 2.41 and 2.42). This submarine volcanic structure was named “Abyssos Crater” because of the great depth of its base around 680 m. The volcanic nature was verified by the analysis of the lithoseismic air-gun profiles showing only very few meters of sediments overlying volcanic formations.

Two representative lithoseismic profiles reveal the neotectonic structure of the Kos-Yali-Nisyros-Tilos volcanic field (Figs. 2.7 and 2.8).

The N-S profile starts from the southern slopes of the Dikeos Mt. on Kos island, showing the northern marginal fault zone and continues through the well-stratified marine and lacustrine sediments and intercalated volcano-sedimentary sequences (e.g. the Kos unidentified incoherent unit, KIU), which is, interpreted as the 161 ka Kos Plateau Tuff deposits (Pe-Piper et al. 2005) of the Eastern Kos Basin and the Eastern Nisyros Rise up to the Tilos marginal fault zone in the south.

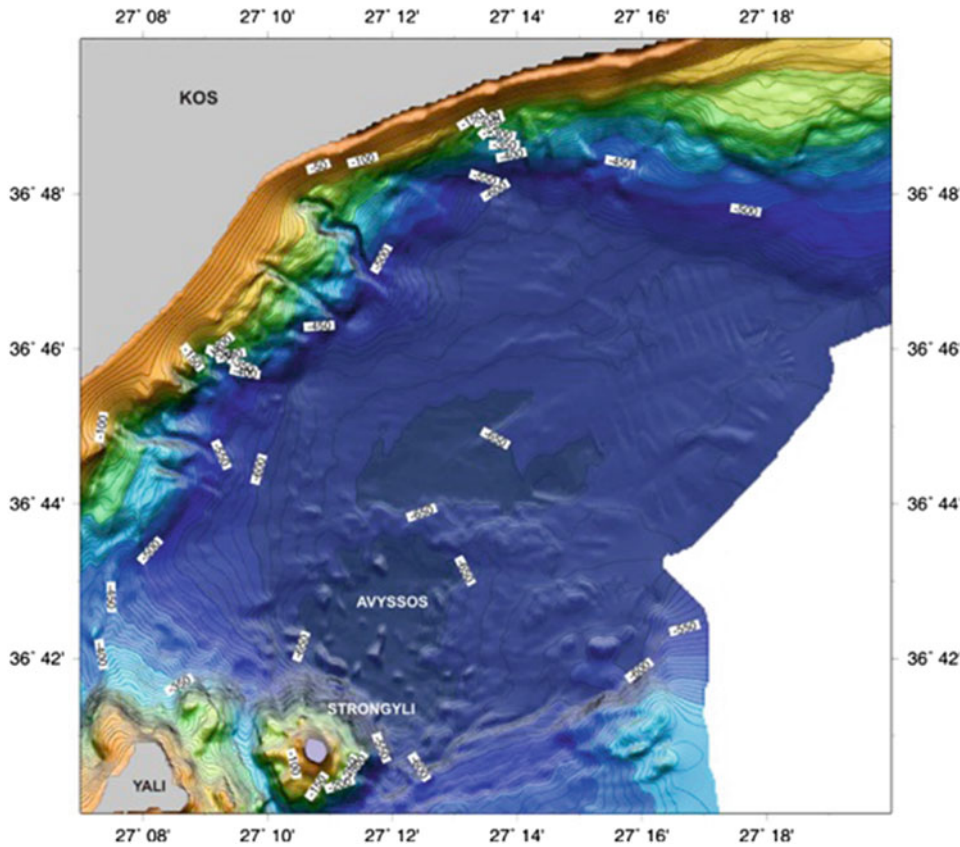


**Fig. 2.6** Detailed bathymetric map of the Eastern Kos Basin using 10 m isobaths. Note the canyons along the northwestern margin and the submarine caldera of “Avyssos” to the northeast of Strongyli islet (Nomikou 2004; Nomikou and Papanikolaou 2010a)

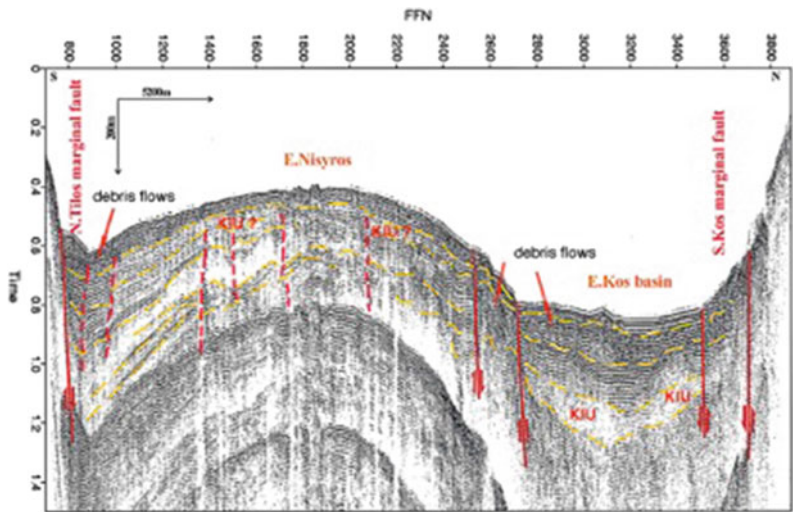


**Fig. 2.7** Representative air-gun S-N profile between Kos and Tilos island through the volcano-sedimentary sequences and intercalated volcanics of the Eastern Kos Basin and the Eastern Nisyros Rise indicating steep marginal NE-SW trending faults (modified after Papanikolaou and Nomikou 2001); *KIU* Kos unidentified incoherent unit interpreted as 161 ka Kos Plateau tuff deposits (Papanikolaou and Nomikou 2001; Nomikou 2004)

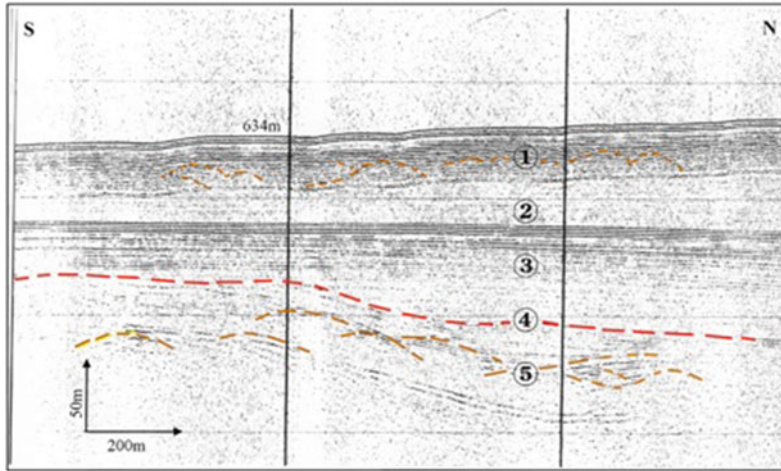


**Fig. 2.8** Representative air-gun N-S profile through the large deep sedimentary Western Kos Basin between Kos and Yali, showing several hundred meters of thick flat-lying sediments (numbers 1–3); modified after Nomikou (2004)

### 2.3.2.2 Western Kos Basin

The Western Kos Basin is bordered to the west by the peninsula of Kefalos and to the north by the southwestern coast of the Antimachia plateau of central Kos (Figs. 2.3, 2.4 and 2.5). Yali islet occurs to the east and Pergousa and Pachia islets to the south. It comprises a volcano-sedimentary sequence of more than 500 m thickness (Fig. 2.8) below its average depth of 520 m and opens towards Eastern Kos Basin to the east, Western Nisyros Basin to the west and Pachia-Pergousa Basin to the south. The continental slopes are abrupt in almost all directions but the western margin towards Kefalos Peninsula is particularly steep and forms an N-S zone of morphological discontinuity.

The deepest part of the basin lies adjacent to the western margin with smooth morphological slopes within the rest of the basinal area, which accumulates radially the sediments towards this subsiding zone. The western margin is controlled by a neotectonic fault of N-S direction, which produces uplift of the western fault-block of the Kefalos Peninsula and subsidence of the eastern fault-block of the Western Kos Basin. The maximum depth of the basin is 530 m and only a small horizontal area can be observed around it of about 1 km<sup>2</sup> area. The southeastern and southern slopes of the basin are reflecting the geometry of the lower part of the volcanic cones of the Yali

and Pergousa volcanoes. At the northwestern part of the basin is observed half of the Kefalos volcanic structure of Middle Pleistocene age (0.5 Ma), with some preserved onshore (Dalabakis and Vougioukalakis 1993) and the rest flowing offshore towards the south. Along the northern slopes of the basin the continental shelf of Kos is observed down to the depth of 150 m. Immediately, below the edge of the continental shelf there is a graduated arc-shaped form of a large landslide, exhibiting a type of radial flow to the south with a morphology of arcuate terraces reaching the depths of 400–450 m. The toe of the sliding mass to the south is confined by the base of the northwestern part of the Yali volcanic cone.

The lithoseismic N-S profiles through the Western Kos Basin (Fig. 2.8) revealed the existence of two major discontinuities, which define successive progradational sedimentary sequences (Papanikolaou and Nomikou 1998). The sequences show vertical displacements up to 100 m due to normal faulting:

- The upper seismic sequence is characterized by parallel seismic reflections with continuous, intense and relatively low-amplitude reflectors, which can be interpreted as relatively coarse-grained sediments reaching 50 m thickness (Fig. 2.8, No. 1).

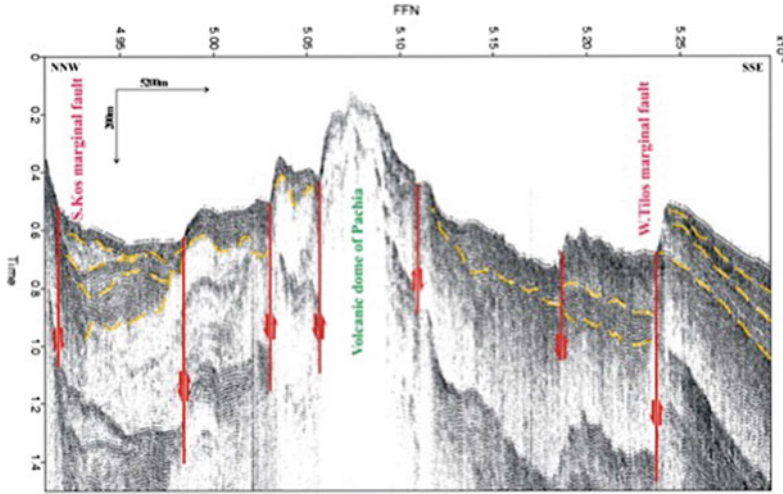


**Fig. 2.9** Representative air-gun NNW-SSE profile between the southern marginal fault of Kefalos peninsula and marginal fault zone of Tilos through the volcano-sedimentary sequence of the western Kos basin,

the Pachia volcanic edifice, and the volcano-sedimentary sequence of the southern Nisyros Basin; strongly elevated; modified after Nomikou (2004)

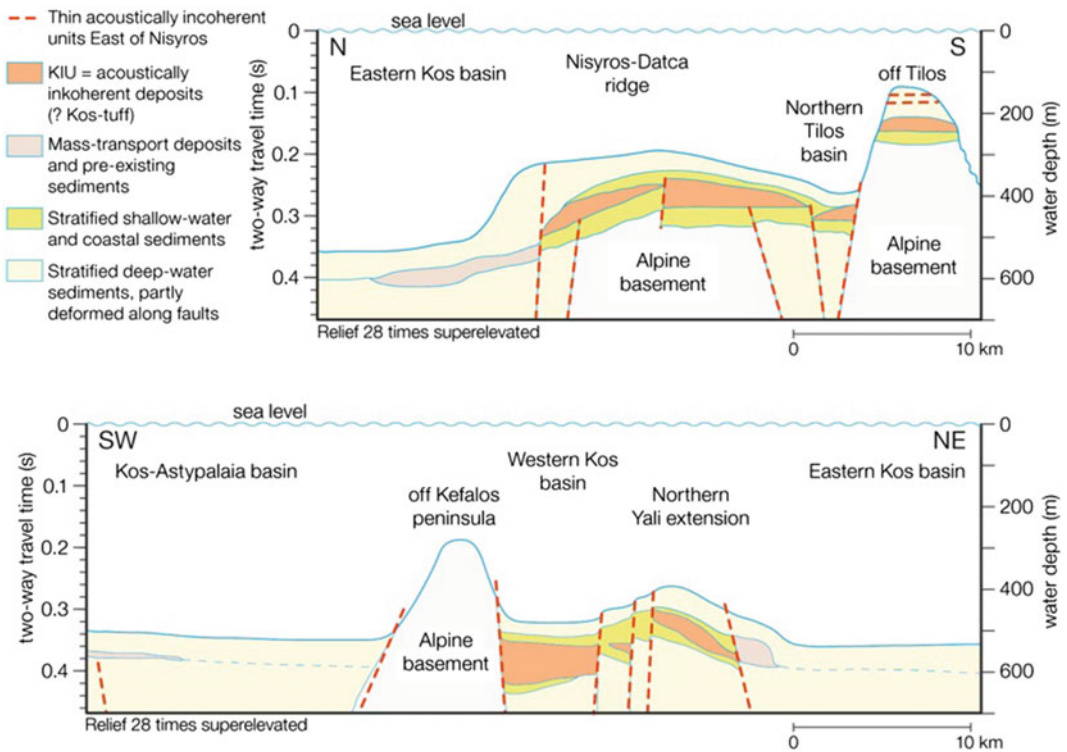


**Fig. 2.10** An interpretative composite cross-section through the sub-seafloor volcano-sedimentary sequences of the west and east Kos basins between the peninsula of Kefalos and Tilos; modified after Pe-Piper et al. (2005)



- The lower seismic sequence (Fig. 2.8, No. 2 and 3) consists of a few weak, discontinuous, subparallel reflectors or reflection free-areas, suggesting fine grained sediment deposition from a relatively quiet environment with a thickness of not more than 200 m.
- A sequence of deformed reflectors (hyperbolic and bulged forms, Nos. 4 and 5, Fig. 2.8) which appear either below the second sequence or emerge from beneath them in some areas between Nisyros and Yali and especially near the island of Strongyli. These reflections may represent volcanic features and possibly volcanic domes. There are no sediments in this region. The volcanic domes emerge from 150 m depth with steep slopes (dip 35–40%).

The NNW-SSE profile between the Kefalos Peninsula and Tilos (Fig. 2.9) shows complex

neotectonic structures in the volcano-sedimentary sequence of the western Kos Basin, the pre-Pleistocene Pachia volcanic lavas, dome south of Nisyros and in the volcano-sedimentary sequence of the southern Nisyros Basin, due to volcanic intrusions and eruptive phases combined with major vertical tectonic displacements (Fig. 2.10).

### 2.3.2.3 Western Nisyros Basin

The Western Nisyros Basin (Figs. 2.3 and 2.4) is bounded by the Kondelioussa tectonic block towards the south and the Western Kefalos Platform (Fig. 2.5) towards the north. Its average depth is 550 m and the volcano-sedimentary thickness below its sea bottom exceeds 600 m. The basinal area is rather flat with maximum depth around 600 m (Fig. 2.11). Its southern margin is characterized by abrupt breaks in slope with steep morphological slopes >20% observed

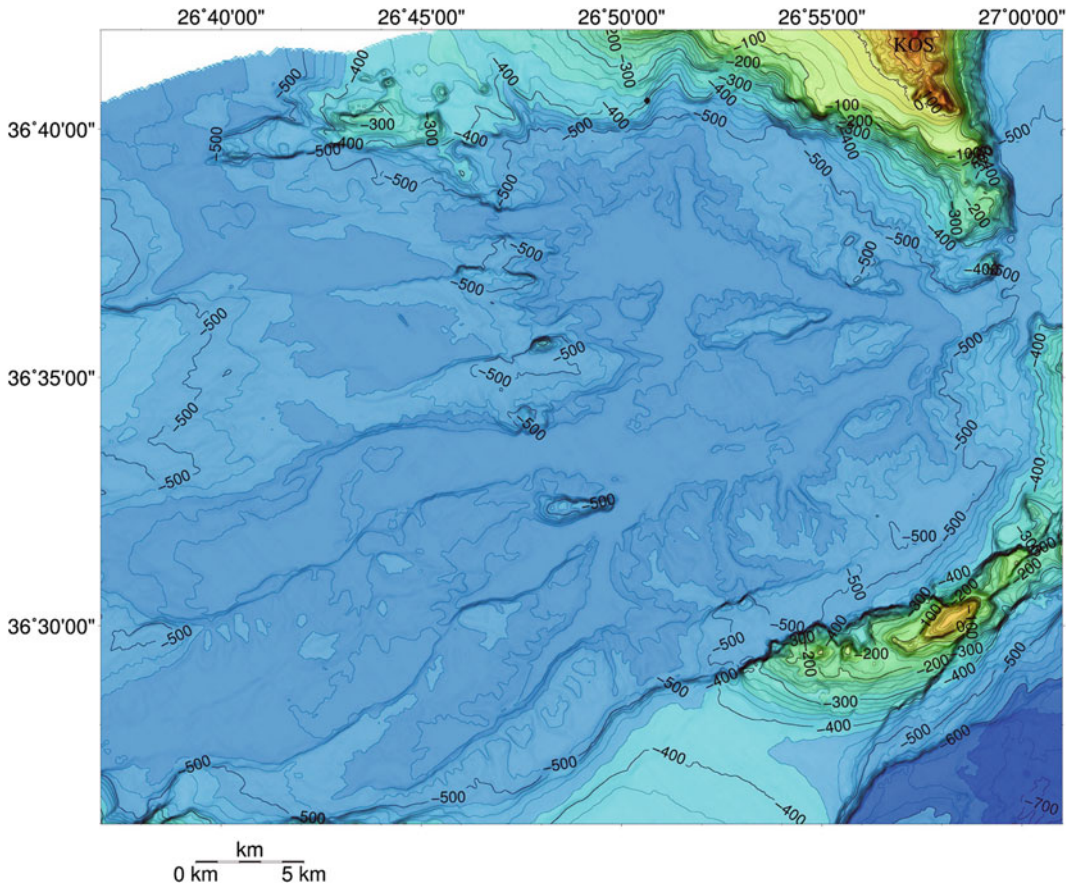


**Fig. 2.11** Bathymetric map of the Western Nisyros Basin using 5 m isobaths. Note the alternation of submarine channels and ridges in the ENE-WSW

direction, the latter being interpreted as volcanic intrusions (Nomikou 2004; Nomikou and Papanikolaou 2010a)



between 500 and 200 m of depth. The basin ends towards the west in the area between the islands of Syrna and Astypalaia. The overall length of the basin is 40–45 km in the ENE-WSW direction and its width is about 15–20 km. The basinal morphology is characterized by a number of flat-floored elongate basins of ENE-WSW direction alternating with parallel ridges, which, according to the air-gun profiles, are interpreted as volcanic intrusions (Nomikou 2004). The northern tectonic boundary of the basin is formed by two intersecting faults of E-W and NW-SE direction separating the tectonic graben from the intermediate marginal blocks and the Kefalos block. This steep morphology is controlled by major fault zone of ENE-WSW direction (Nomikou 2004) separating the uplifted tectonic horst of Kondelioussa islet to the south, which is made of Mesozoic carbonate rocks, from the subsided basinal area to the north.

#### 2.3.2.4 Southern Nisyros Basin

The Southern Nisyros Basin (Figs. 2.3 and 2.12) constitutes the northern end of the large Karpathos basin extending towards the south-southwest, which comprises the eastern segment of the Cretan Basin, which reaches depths of more than 2000 m. The basin is delimited between two major fault zones of NE-SW direction (Nomikou 2004) that have caused subsidence of several hundreds of metres. The two fault zones form the parallel margins of the basin in the NE-SW direction and are characterised by steep slopes. Both marginal faults have produced a strong subsidence of the basin between the uplifted horsts of Kondelioussa in the northwest and Tilos in the southeast. In both horst areas the Mesozoic formations of the Alpine basement are uplifted. A volcanic edifice (? dome) with a small crater has been found during a submersible survey (Fig. 2.13) east of Kondelioussa.

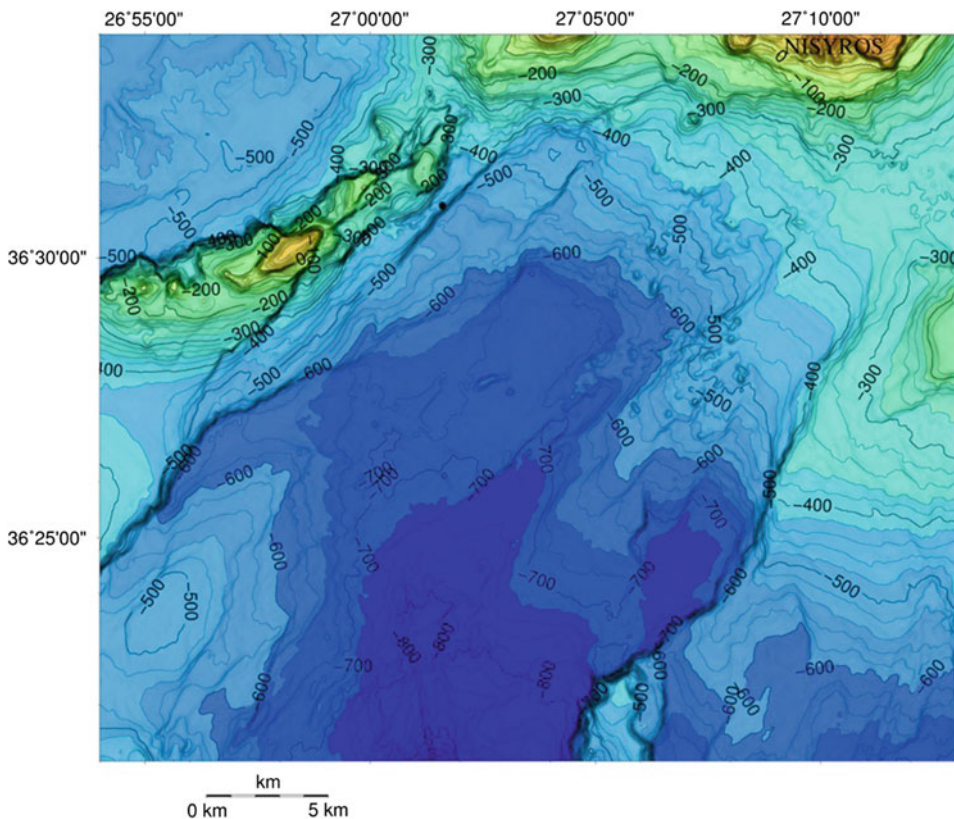


**Fig. 2.12** Bathymetric Map of the Southern Nisyros Basin using 5 m isobaths. Note the submarine volcanic landslides south-southwest of Nisyros and the two steep

marginal fault zones in the NE-SW direction (Nomikou 2004; Nomikou and Papanikolaou 2010a; Nomikou et al. 2013c)

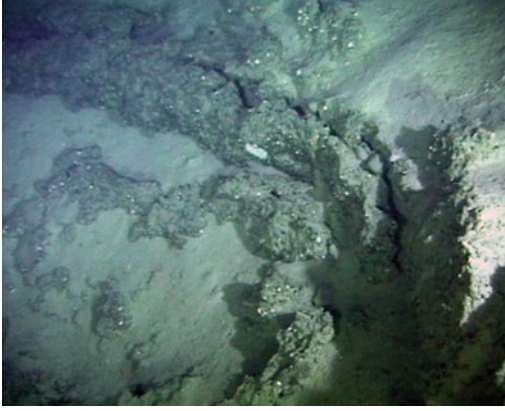


**Fig. 2.13** Edge of volcanic crater (4.5 m diameter and 2 m height) from the volcanic dome east of Kondelioussa at 430 m depths (Nomikou and Papanikolaou 2000; Nomikou 2004; Nomikou et al. 2013a)

The basin is closed towards the northeast by the submarine slopes of the Nisyros volcanic edifice. Hammock morphology, due to several submarine landslides can be observed over a large area of the southwestern Nisyros slopes, e.g. a volcanic debris avalanche reaching 420–680 m of depth (Tibaldi et al. 2008a). The blocks reach 80 m in diameter with different shapes and orientations in a chaotic distribution on the sea floor.

### 2.3.2.5 Pachia-Pergousa Basin

The Pachia-Pergousa Basin is developed within the intra-volcanic area of the Nisyros volcanic field surrounded by the volcanic islets of Pachia to the west, Pergousa to the south and Yali to the north (Fig. 2.14). Nisyros Island borders the

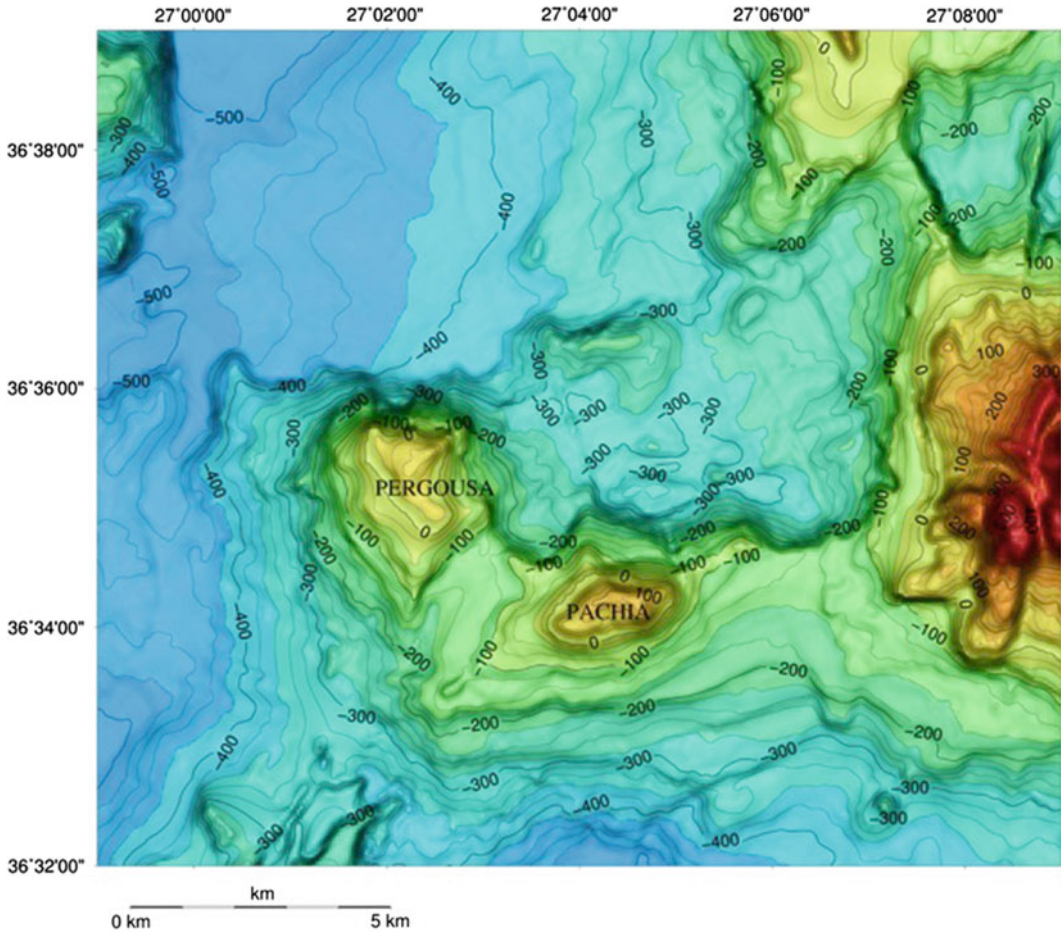


**Fig. 2.14** Bathymetric map of the Pachia-Pergousa Basin using 10 m isobaths (Nomikou 2004; Nomikou and Papanikolaou 2010a)



basin to the east. A number of small fluctuations embossed the seabed likely because of volcanic intrusions. The 300 m isobaths to the north of Pachia delimits the flat part of the basin whose maximum depth reaches 345 m. The slopes to the east and to the south present an abrupt increase of depth shown by dense isobaths due to faults in the N-S and E-W direction. The basin is separated from Western Kos Basin towards the northwest by a ridge of 100 m hypsometric difference, roughly from the isobaths of 300 up to the isobaths of 200 m. Toward east and northeast it is separated from the Yali-Nisyros Basin by a small submarine ridge oriented NNW-SSE at 160 m of depth.

The Yali-Nisyros Basin occurs within the intra-volcanic area of the Nisyros volcanic field and is bordered by Nisyros Island in the south and Yali Island in the north (Fig. 2.15). The basin comprises two sub-basins oriented N-S which are separated by an N-S ridge between Nisyros and Yali islands. The western sub-basin is delimited to the west by the seismic fault zone that was activated in July 1996 and produced extensive damage in Mandraki Town, adjacent to the Panaghia Spiliani Monastery (Nomikou and Papanikolaou 2000). The submarine survey showed a topographic difference across the fault of about 100 m, with the uplifted block to the west at 140 m of depth and the sub-sided block to the east at 235 m depth. The eastern sub-basin

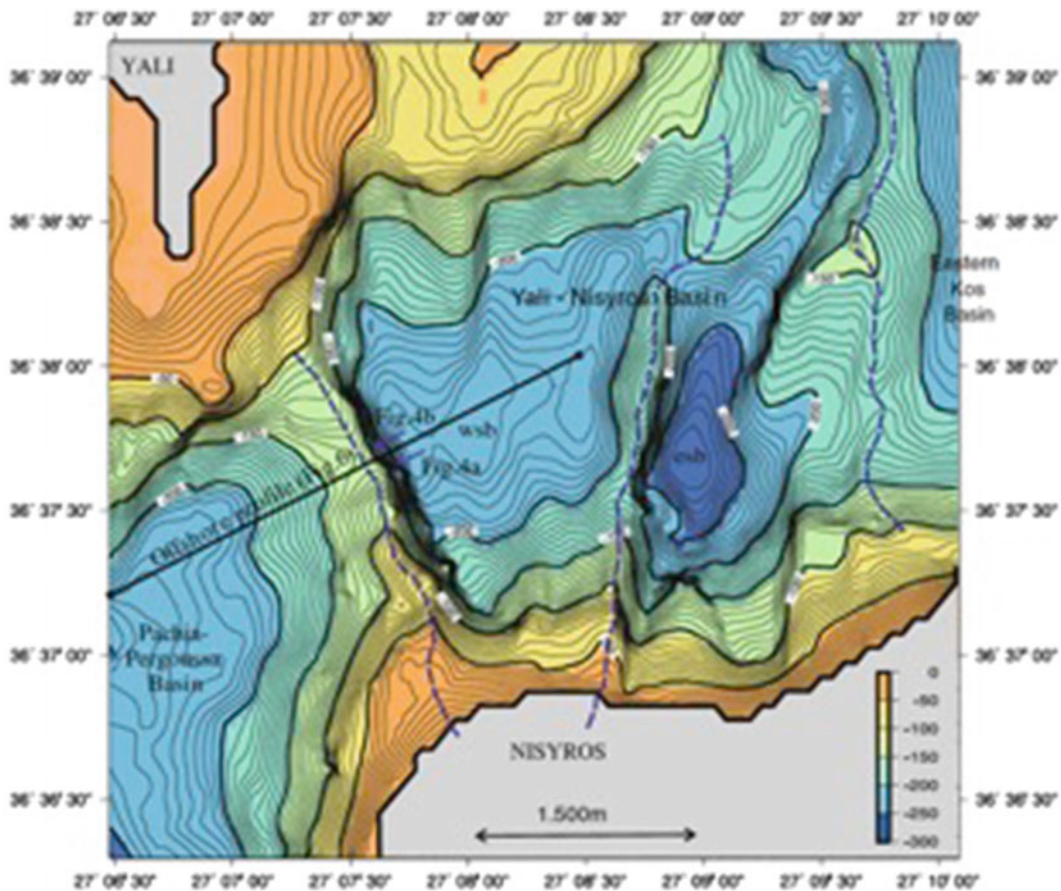


**Fig. 2.15** Bathymetric map of the Yali-Nisyros Basin using 10 m isobaths. Nomikou 2004; Nomikou and Papanikolaou (2011)

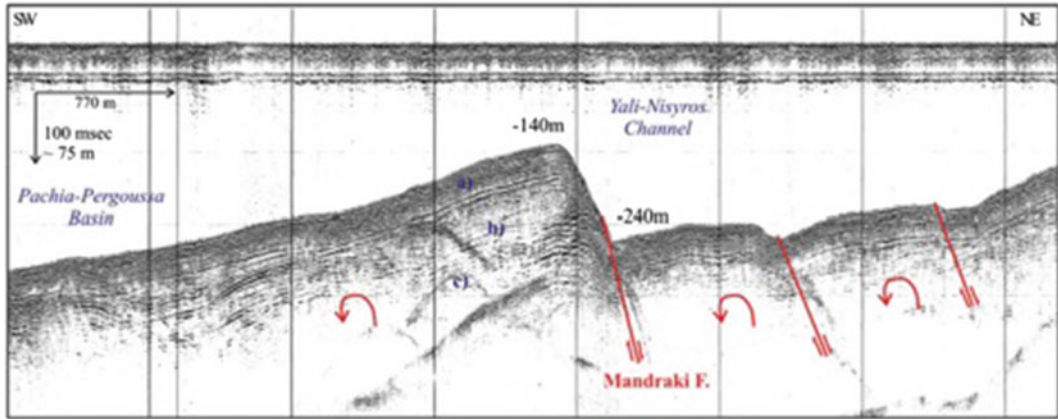


**Fig. 2.16** Representative SW-NE air-gun profile of the small basin between Yali and Nisyros (Fig. 2.16), showing a succession of tilted blocks to the west, associated

with the system of NNW-SSE normal faults (Papanikolaou and Nomikou 2001; Nomikou 2004; Nomikou and Papanikolaou 2011)

is developed also in the N-S direction with deeper maximum depth at 290 m.

Northward extension of the NNW-SSE trending Panagia Spiliani Fault of western Mandraki in the submarine area between Nisyros and Yali. This fault, reactivated during the 1996 earthquakes, caused the damages in the houses and roads of Mandraki exclusively along its strike, without any influence over the rest of the town. The fault throw is estimated on the basis of submarine profiling of about 100 m with an extension of approximately 5 km (Fig. 2.16); Nomikou and Papanikolaou (2000, 2011).

### 2.3.2.6 Tilos Basin

The Tilos Basin is developed to the north of Tilos Island and to the southeast of Nisyros Island (Fig. 2.17). Our map comprises only its western part because of its extension into the Turkish waters towards the east, where it is developed south of the Datça Peninsula. Towards the southeast it terminates in the area north of Simi Island. Towards the north it is bordered from the Eastern Kos Basin by the E-W oriented rise of

Nisyros–Datça. The northern slopes of the basin towards Nisyros Island are smooth, progressively deepening from 300 m to the bottom of the basin at 570 m of depth. On the contrary the southern slopes of the basin towards Tilos Island are more abrupt with dense isobaths and steep slopes >20%. This steep morphological zone is due to a major E-W trending fault zone, developed along the northern margin of Tilos Island. The western part of the basin towards its link to the Southern Nisyros Basin is occupied by a special morphology with numerous hills and longitudinal ridges between water depths of 250 and 380 m. The overall morphology of this area southeast of Nisyros Island can be viewed as a large deposit of volcanic debris avalanche with a seaward termination displaying an irregular pattern characterized by elongated lobes. These lobes and the elongation of the single elevations might represent a series of aligned ridges emplaced parallel to the flow of the debris avalanches from the Nikia rhyolitic volcanic rocks which predated the Nisyros volcano major caldera explosion (Tibaldi et al. 2008a, b; Nomikou et al. 2009).

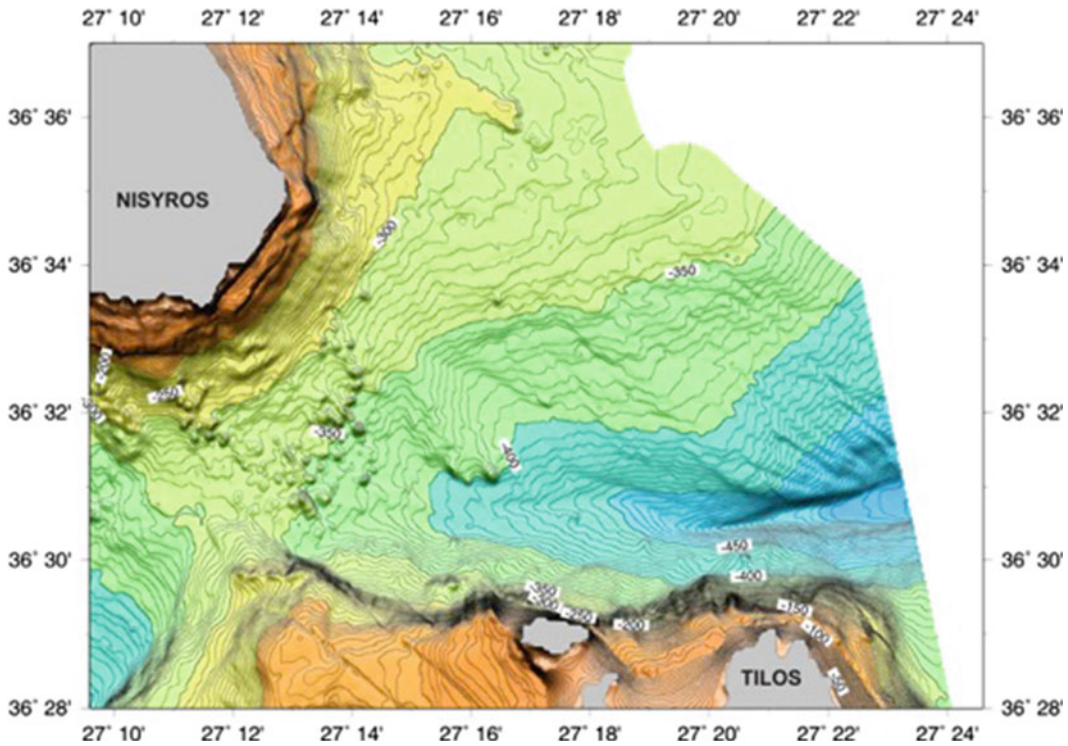


**Fig. 2.17** Bathymetric Map of the Tilos Basin using 5 m isobaths. Note the deposition of the volcanic debris avalanche, which give the seafloor a hammock

topography south of Nisyros; Nomikou 2004; (Tibaldi et al. 2008a; Nomikou et al. 2013c; Livanos et al. 2013)

### 2.3.3 Volcanic Eruptive Centers

#### 2.3.3.1 Kos Island

Kos Island is built up by complex “Stockwerk tectonics”, including Paleozoic metamorphic basement rocks, allochthonous Alpine Mesozoic thrust sheets, a 12 Ma Miocene monzonite intrusion, upper Miocene to Pleistocene volcanics and superficial present-day thermal manifestations (Böger et al. 1974; Böger 1978; Bellon and Jarigge 1979; Keller 1982; Dalabakis 1986, 1987; Bardintzeff et al. 1989; Papanikolaou and Lekkas 1990; Davis et al. 1993; Triantaphyllis 1994; Triantaphyllis and Mavrides 1998; Lagios et al. 1998) that relate to the extensional tectonics in the eastern sector of the island arc. Two major fault systems, ENE–WSW, WNW–ESE, and NNW–SSE faults, led to the present-day structure of the island (Fig. 2.18).

Volcanic activity has been occurring since Late Miocene time in the southern area of Kos

Island (Kefalos Peninsula) and can be divided into two periods (La Ruffa et al. 1999). The oldest volcanics (a trachytic welded ignimbrite) were deposited during the Upper Miocene and are related to a pre-Aegean Volcanic Arc subduction zone (Keller 1982). Pliocene volcanic activity started around 3.4 Ma building dacitic domes (Dalabakis 1987; Keller et al. 1990), and continued between 2.7 and 1.6 Ma with rhyolitic domes, the pyroclastics of the Kefalos tuff ring (Francalanci et al. 2005; Allen et al. 2009) and the Zini perlitic obsidian dome. Later activity may have caused the small caldera collapse of the Kamari Bay (Dalabakis and Vougioukalakis 1993; Francalanci et al. 2005). Plinian type eruptions produced large volumes of rhyolitic ignimbrites over a time span of 10 million years and terminated in the largest event 161,000 years ago with 100 km<sup>3</sup> of magma deposited as ignimbrites and ashes (“Kos Plateau Tuff”: Stadlbauer 1988; Allen 2001; Bachmann 2010).



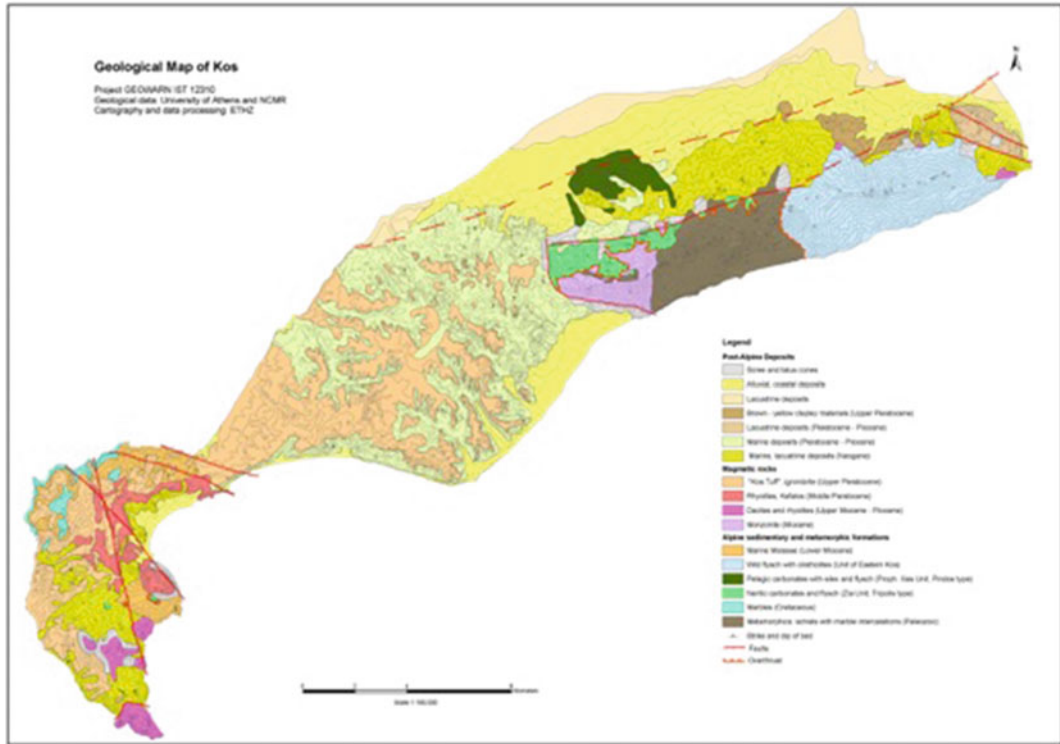


**Fig. 2.18** Simplified geological map of Kos island after Nomikou (2004)

### 2.3.3.2 The Kos Plateau Tuff

The largest volcanic deposit of the Kos-Nisyros area (the Kos Plateau Tuff, hereafter KPT, Figs. 2.18, 2.19, 2.20, 2.21, 2.22, 2.23, 2.24 and 2.25) erupted ~161 k.y. BC (Ar-Ar dating; Smith et al. 1996), generating >60 km<sup>3</sup> of non-welded rhyolitic ash and pumice (Keller 1969; Allen 1998, 2001; Pe-Piper et al. 2005; Bachmann et al. 2010) covering an area ~5000 km<sup>2</sup> (Stadlbauer 1988). The young age of deposits, and their excellent preservation in the dry Mediterranean climate provides an exceptional opportunity to dissect such a unit using the latest analytical techniques in petrology and geochemistry. The KPT is best preserved on Kos, but is also exposed on the neighbouring Greek islands of Tilos, Kalymnos, Pachia and on the Turkish peninsula of Bodrum and Datça (Allen 2001). Isopach (Fig. 2.20), isopleths and transport direction data indicate that the vent areas for the KPT were situated in the bay between southwest Kos and Nisyros volcano. The eruption

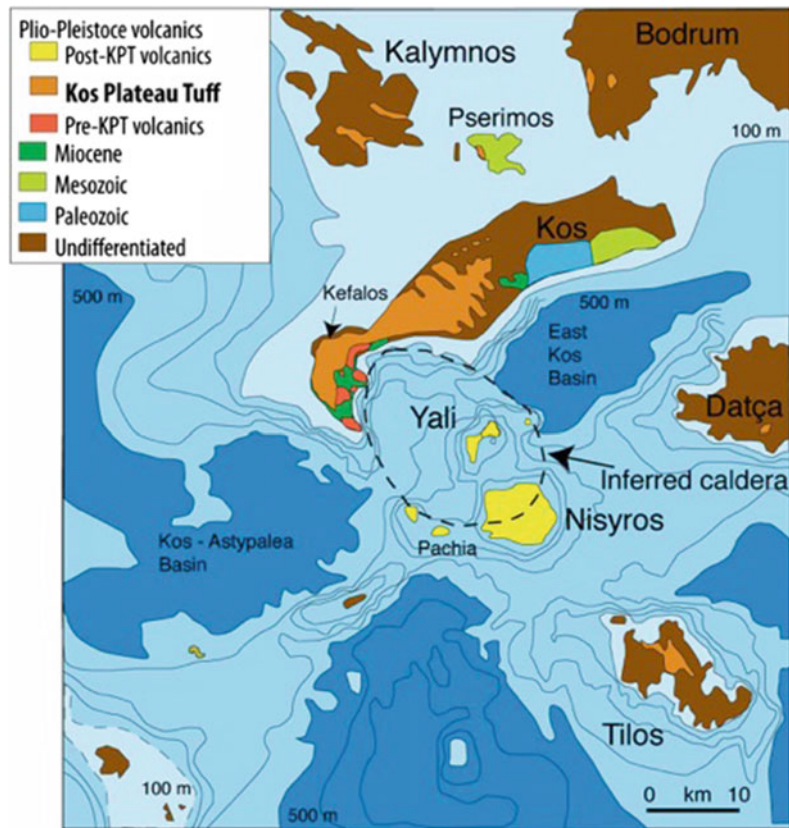
is inferred to have formed a caldera at least 6–11 km in diameter, and perhaps as much as 20 km (Allen 2001; Pe-Piper et al. 2005).

Ash-layers are found in deep-sea sediments 500 km southeast of Kos, near Cyprus (W-3 deep sea ash layer, Federman and Carey 1980). The source of this eruption and caldera can be inferred on the basis of the distribution of extensive lag deposits as between the present southeast Kefalos/Kos coast and the islets of Pergousa and Pachia in the area of the present day island of Yali in the Pachia-Pergousa Basin.

A presumed large flooded caldera in this area has been probably obliterated by post caldera activity. Younger eruptions, which built up Nisyros and Yali volcanic islands, as well as tectonic uplift and downfaulting in the complex horst-graben system have changed the original morphology of the environment.

The KPT eruptive stratigraphy has been studied in detail by several authors (Allen 1998, 1999, 2001; Allen and Cas 1998a, b; Allen and McPhie 2001).

**Fig. 2.19** The Pleistocene (Calabrian) Kos Plateau Tuff (KPT) covered an area of  $\sim 5000 \text{ km}^2$  with pumice flows; modified after Pe-Piper et al. (2005) and Bachmann (2010)



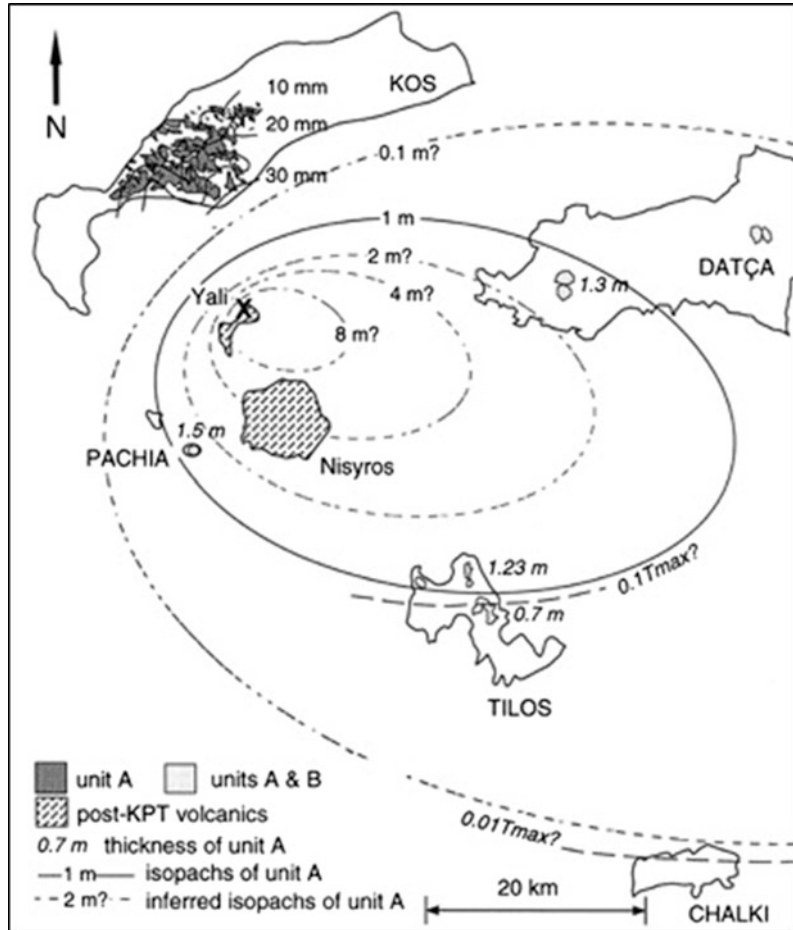
The eruption began and ended with phreato-plinian activity (Units A, B and F in Figs. 2.21, 2.24 and 2.25; Allen and Cas 1998a; Allen 2001). As the eruption waxed, the style of activity changed to magmatic-volatile-driven, with the generation of relatively widespread, topographically-controlled ignimbrites (Unit D). Most of the volume was erupted during the climactic caldera-forming phase, which produced a widespread, highly energetic pyroclastic flow (Unit E). The change in fragmentation style from phreato-plinian to pre-climactic and climactic is recorded in the morphology of the pumice clasts and ash shards.

The KPT is a non-welded pyroclastic deposit, consisting of juvenile components (pumice clasts, glass shards, crystal fragments) and lithic fragments (some up to 3–4 m in diameter) from different provenance (mainly andesite to dacite clasts, but also rare occurrences of schist, metabasalt, sandstone, limestone and rhyolite; Smith et al. 2000; Allen 2001). During the climactic part

of the eruption (unit E, Fig. 2.23), granitic clasts, some containing 10–20 vol.% interstitial melt, were also erupted. These are juvenile, or co-magmatic clasts, as they have the same zircon age range as the pumice samples (Bachmann et al. 2007). Several types of pumices can be distinguished on the basis of macroscopic characteristics (Allen 2001). Three petrologic useful categories can be isolated: (1) crystal-rich pumice (comprising both tube and frothy pumices), (2) crystal-poor pumices, and (3) banded (or grey) pumices. The texture, whole-rock composition, and mineralogy of each type of juvenile clasts are detailed below (see Electronic Supplementary Material Appendix 1 for pictures of thin sections and hand samples of all four pumices in the KPT).

Crystal-rich pumices have crystal contents between  $\geq 25$  and 35 vol.% crystals (Bouvet de Maissonneuve et al. 2008) and by far dominated the clast assemblage ( $>99\%$ ). Crystal-poor pumices ( $<5$ –10 vol.% crystals), while the are

**Fig. 2.20** The Kos Plateau Tuff: regional distribution of the pyroclastic deposits A and B, and extrapolated isopachs of unit A. Units A and B cover the central Kos plateau north of the inferred vent X in the area of Yali. Unit A occurs also south and east of the vent on Pachia, Tilos and the Datça peninsula. The 1 m and 30, 20 and 10 mm isopachs of unit A are shown, along with the inferred 0.1, 2, 4, and 8 m isopachs. Estimated 0.1 and 0.01 Tmax are also shown. Copyright note modified after Allen and Cas (1998a)



only found in the early parts of the eruptions (subunits A and B), while grey and banded pumices can be found throughout the eruption sequence, although they are more conspicuous in units D and E (Bachmann 2010). The main mineral phases are, in decreasing order of abundance; plagioclase, quartz, sanidine, and biotite. Some pyroxene and rare olivine can be found in grey and banded pumices (Piper et al. 2010). Accessory phases include Fe–Ti oxides, apatite, zircon and monazite.

Many juvenile, granitic enclaves, can be found in the KPT (mostly in unit E: Keller 1969; Allen 2001; Bachmann 2010). These granitic enclaves are texturally variable (Bachmann 2010); most contain glass at the boundaries between minerals (that has vesiculated, making samples very friable) but others are holocrystalline (no interstitial

melt). The enclaves show a textural gradation from coarse-grained (with mm-sized crystals) to fine-grained, through intermediate bimodal textures. Enclaves are typically finer-grained holocrystalline, suggesting more rapid cooling. When interstitial melt is present, it is mainly located at the grain boundaries, forming meandering channels. In some places, crystals faces are found against glass, suggesting late growth from a residual melt rather than partial melting. Melt content varies from 0 to ~40 vol.%, (Keller 1969; Bachmann 2010).

Combined textural, petrologic and geochemical information (Bachmann et al. 2007; Bachmann 2010) suggest that (1) the system evolved dominantly by crystal fractionation, with limited amounts of crustal assimilation, from (mostly non erupted) more mafic parents, (2) the magma

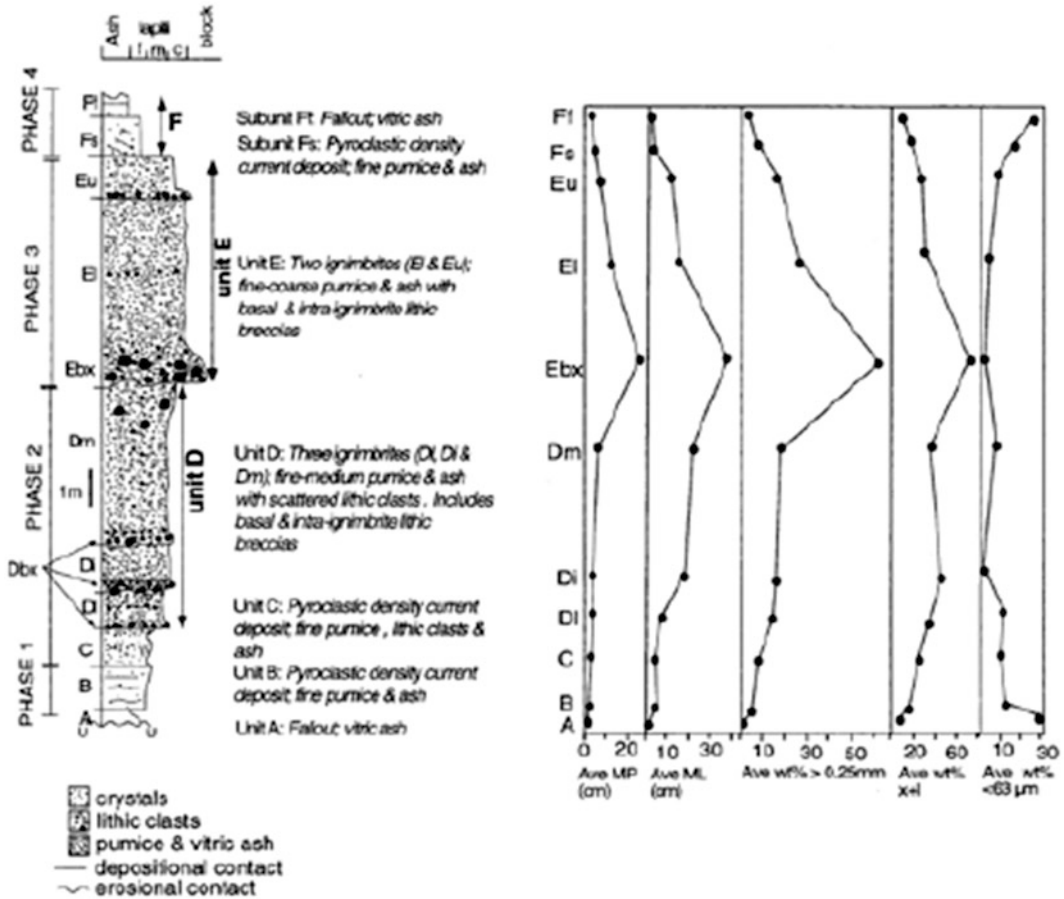


**Fig. 2.21** Composite graphic stratigraphic log of the KPT from showing the six units and four eruptive phases of the KPT. 'Dry' refers to the dry magmatic

volatile-driven explosive phases and 'wet' refers to the phreatomagmatic phases. Copyright note Allen et al. (1999)

reservoir grew over  $\geq 250,000$  years at shallow depth ( $\sim 1.5\text{--}2.5$  kb) and magma was mostly stored as a volatile-rich crystalline mush close to its solidus ( $\sim 670\text{--}750$  °C), (3) the eruption occurred after a reheating event triggered by the intrusion of hydrous mafic magma at the base of the rhyolitic mush. Rare banded pumices indicate that the mafic magma only mingled with a trivial portion of resident crystal-rich rhyolite (Piper et al. 2010); most of the mush was remobilized following partial melting of quartz

and feldspars induced by advection of heat and volatiles from the underplated, hotter mafic influx, as is commonly seen for crystal-rich rhyolite deposits in many volcanic provinces around the world (Pallister et al. 1992; Nakamura 1995; Murphy et al. 2000; Couch et al. 2001; Bachmann et al. 2002; Molloy et al. 2008; Cooper and Kent 2014; Kiss et al. 2014). Figures 2.3, 2.24 and 2.25 represent various outcrops along the southern coast of Kos Island between Kefalos and Kardamena.



**Fig. 2.22** The Pleistocene “Kos Plateau Tuff” seen from south (Kefalos). In the foreground Kamari beach and the islet of Kastri (ignimbrite relict). In the background the 161,000 years ignimbrites of the Kos plateau; Mount Dikeos (842 m) in the far background. *Photo V. Dietrich*



**Fig. 2.23** The “Kos Plateau Tuff” on *top* of the Pliocene pumice deposits hillside of Kefalos (north of the upper village of Kamari), which constitutes unit E in the upper 10–15 m *top*, however with limited unit D, units A and B missing (Stadlbauer 1988). *Photo V. Dietrich*







**Fig. 2.24** The “Kos Plateau Tuff” exposed in an isolated up to 100 m high table mountain west of Kardamena close to the southern coast of Kos island, presumably representing the most proximal facies near the original source. Units A to D representing the 1st and 2nd cycles of the eruption are present: units A and B form the base,

covered with vegetation, C and D constitute the monumental *upper part*, C being a 8 m thick wavy-massive non-welded ignimbrite, overlain by 8 m thick fine-grained ignimbrite, which passes into a massive lithic-rich ignimbrite facies at the *top*; characterised by the erosional holes. Photo V. Dietrich



**Fig. 2.25** Detail of the transitional zone between units A, B and E in the central part of Kos island (roadcut through the Plaka forest approximately 2 km west of the airport). 1–2 m of unit B is represented by fine wavy-stratified facies, discordantly overlain by an ignimbrite containing lithics of varies size at the base. Photo V. Dietrich

### 2.3.3.3 Nisyros Volcanic Field

The submarine region of Nisyros, extending from Kos in the north to Tilos in the south, constitutes a large tectonic graben divided into several basins with 600 m average depth (Fig. 2.26). This basin

is penetrated by a complex volcanic group forming the volcanic islands of Nisyros, Pachia, Pergousa, Yali and Strongyli and small intra-volcanic basins with less than 350 m of depth. The volcanic formations are found at 680 m depth (Abyssos in the Eastern Kos Basin) and at the eastern base of the Strongyli volcanic cone up to 700 m of altitude (rhyodacitic domes of Prophitis Ilias on Nisyros) creating a total volcanic relief of more than 1400 m (Nomikou and Papanikolaou 2011). This middle zone with an ENE-WSW general trend from Kondelioussa in the west to Datça Peninsula to the east represents an uplifted tectonic horst above sea-level, the pre-Pleistocene Alpine basement in Kondelioussa Island together with a voluminous cover of volcanic and volcano-sedimentary rocks of the Nisyros volcanic field, separating the large graben zone into two adjacent grabens to the north and to the south. Such a large, recent volcano-morphological situation demonstrates the powerful geodynamic processes of the eastern edge of the active South Aegean Volcanic Arc.

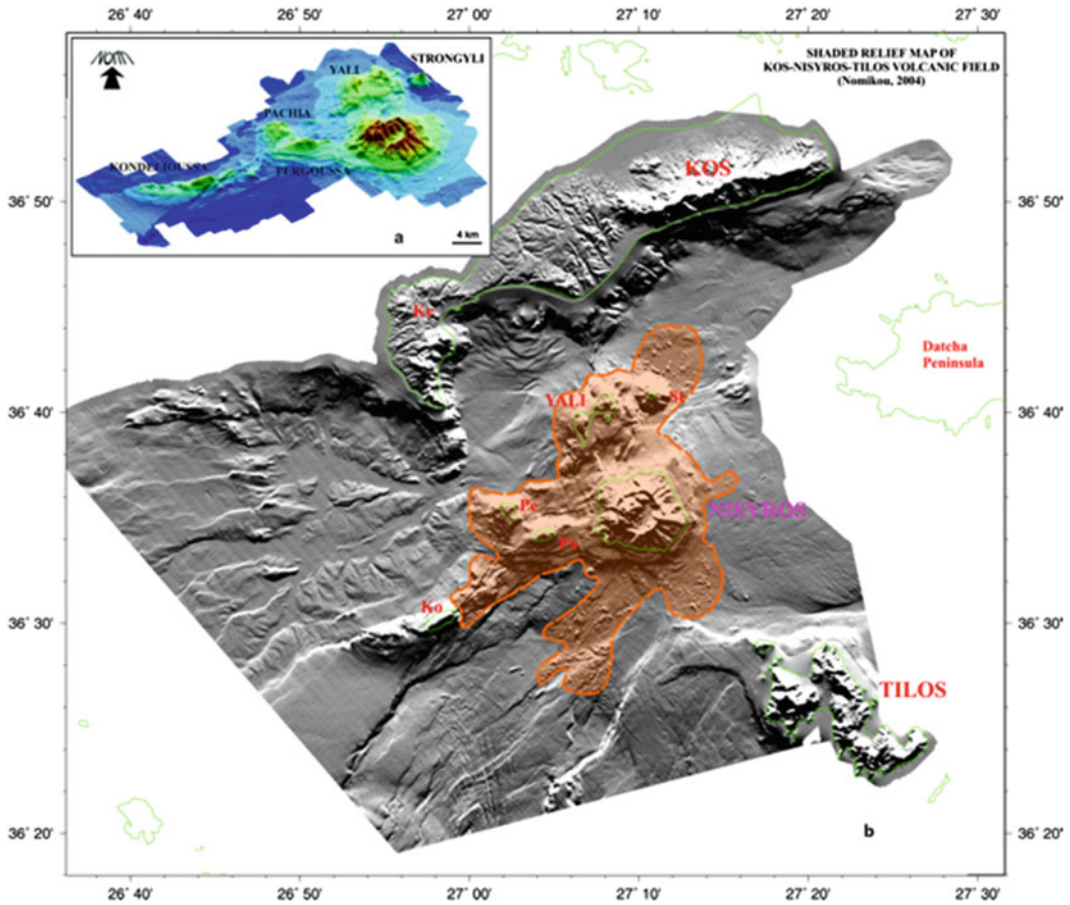


**Fig. 2.26** Shaded onshore and offshore topographic relief map of the Kos-Yali-Nisyros Volcanic Field based on data obtained from multi-beam bathymetric survey during 2000–2002 and combined with onshore hypsometric data. The volcanic outcrops and the resulting

volcanic relief around Nisyros volcano are contoured by orange line. *Ko* Kondelioussa, *Pe* Pergoussa, *Pa* Pachia, *St* Strongyli, *Ke* Kefalos; (Nomikou 2004; Nomikou and Papanikolaou 2010b; Nomikou et al. 2013a)

A number of volcanic centers exist around Nisyros (Fig. 2.26), which developed within the neotectonic graben, in shallow areas. These are: (1) The Nisyros caldera with a top of the rim at +580 m and a bottom at +80 m; (2) The Yali volcanic cone which exhibits a partly submerged caldera (bottom  $\approx$  300 m, top +170 m); (3) The Strongyli volcanic cone, which starts from 650 m depth of the seafloor up to +120 m; (4) The submarine Avyssos Crater northeast of Strongyli in the depth of  $\approx$  670 m up to  $\approx$  590 m; (5) The Pergoussa volcanic cone (bottom  $\approx$  400 m, top +100 m); (6) The domes of Prophitis Ilias (bottom  $\approx$  270 m, top +698 m);

(7) The volcanic domes of Pachia islet (bottom  $\approx$  250 m, top +150 m); (8) The submarine volcanic domes to the east of Kondelioussa islet (bottom  $\approx$  400 m, top  $\approx$  80 m).

#### 2.3.3.4 Yali Island

The Yali volcanic island, an Upper Quaternary rhyolitic edifice with a max. altitude of 165 m, is located north of Nisyros Island and exhibits parts of a submerged caldera which are dissected by a post-caldera N-S fault (Figs. 2.27 and 2.29). Yali seems to represent the youngest volcanic centers of the Nisyros volcanic field. The south-western part of the island is made of two pumice



**Fig. 2.27** Aerial view from northeast of the *hourglass shaped* island of Yali. In the *background* the stratigraphically older part made up by the voluminous rhyolitic pumice deposits, in the *foreground* the Kamara perlitic obsidian dome and flows covered by pumice breccia and

pyroclastic fallout; in the southern part the isolated islet of Ag. Antonios (Fig. 2.33), which consists of an andesitic lava covered by a thin paleosol, reworked lower pumice and Kamara pyroclastics. *Photo* Snipe view Wikipedia



**Fig. 2.28** The Yali pumice deposits are exposed as 60–100 m high cliffs, dipping 10° towards SW and comprise a minimum volume 0.3 km<sup>3</sup>, with the base and submarine portion unknown. The deposits are dissected by normal

faults with max. Displacement of up to 100 m: dominantly trending NW–SE and subordinately E–W and NE–SW (Fig. 2.29). *Photo* V. Dietrich

successions, the “Lower and Upper Pumice” (Figs. 2.28 and 2.36), divided by silty sandstones, whereas the north-eastern part of Yali comprises rhyolitic obsidian-perlitic lava domes and flows at 24 Ka (Wagner et al. 1976), which are locally covered by pumice deposits, equivalent to the upper pumice of western Yali. Marine

terrace deposits, rich in clasts of the Lower Pumice and marine fossils in calcite cement separate these two volcanic parts of the island (Fig. 2.29).

The islet south of Yali, Ag. Antonios (Figs. 2.29, 2.36, 2.37 and 2.38) is built up by gray dacitic porphyritic lavas, with phenocrysts



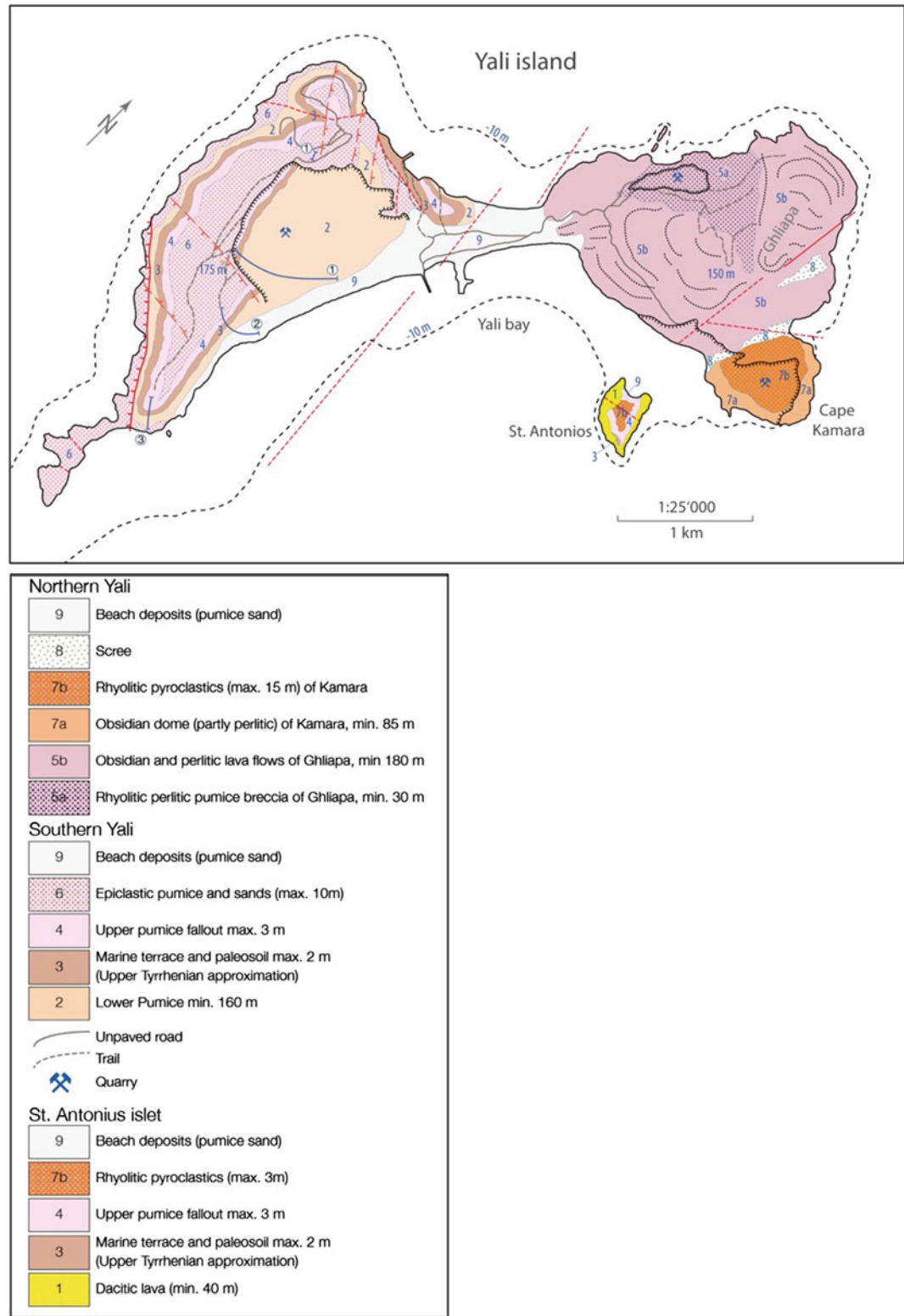


**Fig. 2.29** Geological map of Yali Island and Ag. Antonios islet (geology redrawn and modified after “Nisyros sheet”, geological map of Greece 1:25,000, IGME 2003). Blue lines with encircled numbers 1, 2 and 3 from north to south refer to lithostratigraphic columns of Fig. 2.36 (Allen and McPhie 2000)





**Fig. 2.30** Obsidian flow (7a) overlain by rhyolitic breccias (Fig. 2.40) and topped by a pyroclastic pumice fall and surge succession (7b) in the eastern coastal cliffs of Cape Kamara Yali. Photo V. Dietrich



**Fig. 2.31** Obsidian flow (7a) overlain by rhyolitic breccias and topped by a pyroclastic pumice fall and surge succession (7b) in the southern coastal cliffs of Cape

Kamara Yali; buildings: perlite exploitation and processing company. In the background the Ghilapa obsidian flow (5b). Photo V. Dietrich

of plagioclase, clinopyroxene, orthopyroxene, and magnetite, rich in andesitic enclaves.

The rhyolitic obsidian-perlite lavas and small endogenous domes of Kamara (Figs. 2.30, 2.31 and 2.32) contain sparse phenocrysts of plagioclase, hornblende, biotite, corroded quartz and magnetite and are covered by up to 8 m of bedded fallout deposits with parallel horizons of angular lapilli and ash of perlitic aphyric pumice. Phenocrysts are plagioclase, hornblende, clinopyroxene, biotite and magnetite (Figs. 2.34 and 2.35).

Allen and McPhie (2000) divided the Yali pumice breccia into a “Lower Pumice” of submarine origin and into an “Upper Pumice” of subaerial origin. The transition between the two major units and the detailed lithostratigraphy of

the Upper Pumice is shown in Fig. 2.30, as well as in the outcrop photographs (Figs. 2.36, 2.37 and 2.38).

The white, rhyolitic, aphyric “Lower pumice breccia”, varying in size from coarse ash to boulder, moderately-well sorted and diffusely-stratified reaches an outcropping thickness of 150 m. The larger clasts are prismatic with quenched surfaces and internal polyhedral joints. The smaller pumice clasts, although compositionally, texturally, and prismatic, lack the quenched surfaces. Characteristic minerals of the white pumice are rare microphenocrysts of plagioclase and corroded quartz, whereas a rare percentage (3–5%) of gray pumice contains abundant microphenocrysts of plagioclase, clinopyroxene, orthopyroxene, hornblende and

**Fig. 2.32** *Upper part of rhyolitic obsidian lava and breccia at the southern shore of Kamara. Photo V. Dietrich*

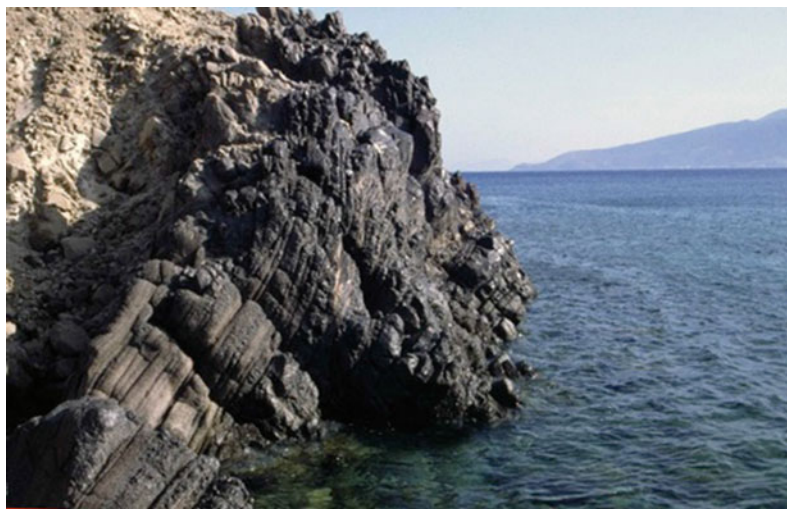


**Fig. 2.33** *Ag. Anthonios islet, view from North. The base is made up of at least 40 m dacitic lava, covered by 3 m of upper pumice fallout (above beach) and thick rhyolitic pyroclastics. Photo V. Dietrich*



magnetite. These deposits are gradationally overlain by a 0.3 m thick, fossiliferous limestone and by a sandy brownish bioclastic sandstone (Fig. 2.38).

The  $\leq 3$  m thick well-sorted and cemented angular fallout lapilli of the “Upper Pumice” is comprised of white (70%) and gray pumice and obsidian fragments. Microphenocrysts are plagioclase, hornblende, clinopyroxene and magnetite, as well as rare muscovite and quartz. Federman and Karey (1980) assumed an age of 31 Ka correlating the Upper pumice with a tephra horizon in deep-sea sediment cores. The paleosol is covered by redeposited epiclastic

pumice in a shallow marine environment containing rounded clasts, subangular obsidian fragments, and shells. The uppermost part turns into a sandy paleosol, rich in ceramic potshards and obsidian blades, witnesses of a Neolithic settlement on the island.

Allen and McPhie (2000) proposed for the Yali pumice breccia formed via a submarine phreatomagmatic eruption (Fig. 2.39): The lavas extruded with phreatomagmatic explosions and passive disintegration of large quenched pumice clasts. Deposition occurred continuously and involved simultaneous resedimentation from a more proximal site on the seafloor.

**Fig. 2.34** Quarried rhyolitic breccia, partly perlitic, at the top of the large obsidian flow in the northern part of Kamara. *Photo V. Dietrich*



**Fig. 2.35** White and gray pumice fallout deposits at Kamara containing interbedded fine ash layers and layers of angular perlitic pumice lapilli, which are exploited. *Photo V. Dietrich*



None of the underwater slopes of Yali had been explored prior to the Nautilus cruise NA011 in 2010. The ROV Hercules was used to explore the eastern flank of Yali identified on the multi-beam map of the area (Nomikou 2004). The outcrops of volcanic rocks at the sea bottom are covered by heavy encrustations or by biogenic

and concreted layers. ROV exploration of the eastern flank revealed spectacular wave type structures in the sediments on the seafloor (ripples) with dark sediments on the ridges of the undulations and light sediments in the troughs (Figs. 2.15 and 2.16). Some linear fractures were explored at various depths (Nomikou et al. 2011).



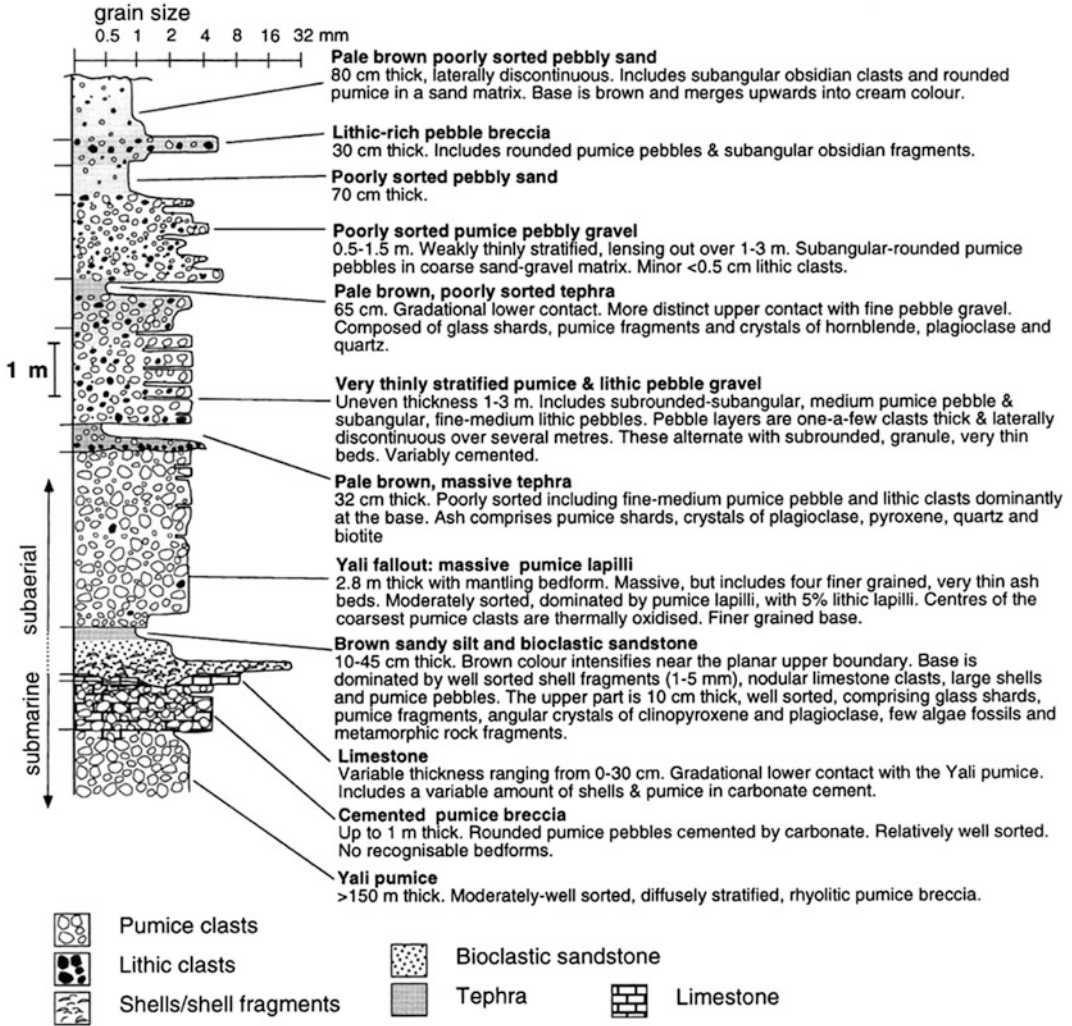


**Fig. 2.36** Copyright note Lithostratigraphic columns through the upper part of the Yali pumice breccia at cross section 3 (Fig. 2.29) and the overlying sedimentary and volcanic units after Allen and McPhie (2000). The

sequence represents an upward progression from submarine to subaerial depositional environments. Locality in the uppermost southwestern parts of the pumice quarries (Figs. 2.29, 2.37 and 2.38)





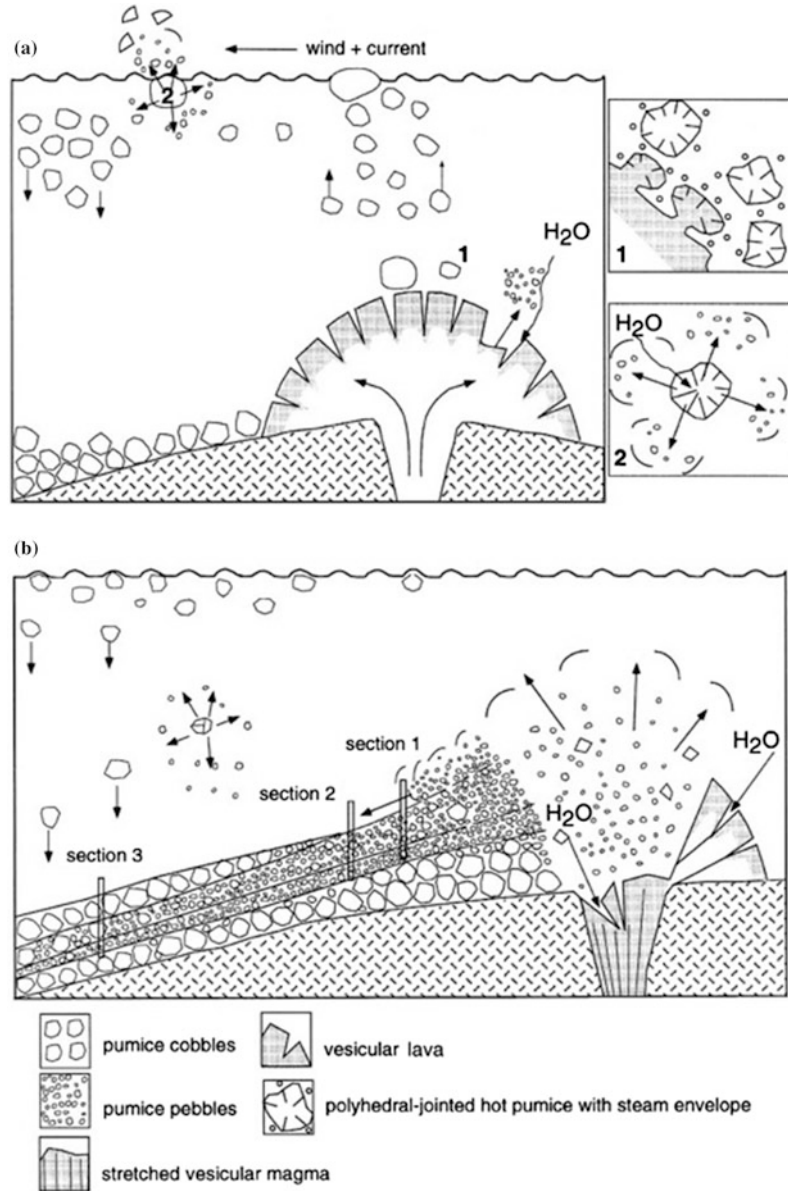
**Fig. 2.37** Transitional zone between the *lower* and *upper* pumice sequences close to the *top* of the southwestern quarry walls (Figs. 2.28 and 2.29). From *bottom* to *top*: approximately 2 m of “lower pumice breccia”, 1 m of *white* cemented pumice breccia, up to 0.5 m of *brown* sandy silt and bioclastic sandstone, up to 3 m of *white* “Yali fallout” of pumice lapilli with thin ash beds, and up to several meters

of poorly sorted reworked pumice pebble gravel including lithic clasts. The *top* is covered by redeposited epiclastic pumice from a shallow marine environment containing rounded clasts, subangular obsidian fragments, and shells and passes up into a sandy paleosol, rich in ceramic pot shards and obsidian blades, witnesses of a Neolithic settlement on the island. *Photo* V. Dietrich

**Fig. 2.38** *Brown* sandy silt and sandy *brownish* bioclastic sandstone dividing the *lower* and *upper* pumice sequences (see Fig. 2.36), unconformably overlain by *white* “Yali fallout” of pumice lapilli; locality close to the *top* of the southwestern quarry walls. *Photo* V. Dietrich



**Fig. 2.39** *Copyright note*  
Submarine eruptive and depositional model for the generation of the Yali pumice breccia (Allen and McPhie (2000). **a** Shallow submarine effusive state with dome formation including simultaneous degassing, vesiculation, expansion and fragmentation of rhyolitic lava; **b** during pulses of stronger magma ascent and degassing explosive phreatomagmatic activity occurred creating an unstable apron of smaller pumice clasts that was continuously subjected to downslope resedimentation by gravity flows



### 2.3.3.5 Strongyli Volcano

The Strongyli volcanic cone is located north of Nisyros emerging from 650 m depth at the sea-floor with a diameter of 3.5 km and reaching the top of Strongyli islet at 125 m above sea level (Fig. 2.40). Its ideal cone-shaped morphology with up to 50° steep flanks contains a 300 m wide crater at the top. At 50 m altitude conglomerates indicate recent uplift. The entire edifice is made

up of gray andesites and minor pyroclastics. The age of formation is unknown, but must be older than the Yali edifice, since rhyolite pumice from Yali with up to 2 m thickness occurs in several morphological depressions and pockets.

Submersible dives with Thetis of Hellenic Center for Marine Research (HCMR) in 2000 in the NW flank of the volcanic cone discovered an underwater crater of several meters of diameter



**Fig. 2.40** The Strongyli volcanic cone seen from southeast. The broken flank exhibits highly oxidized reddish lava surfaces at lower levels. Pyroclastic deposits cover the upper slopes. *Photo V. Dietrich*

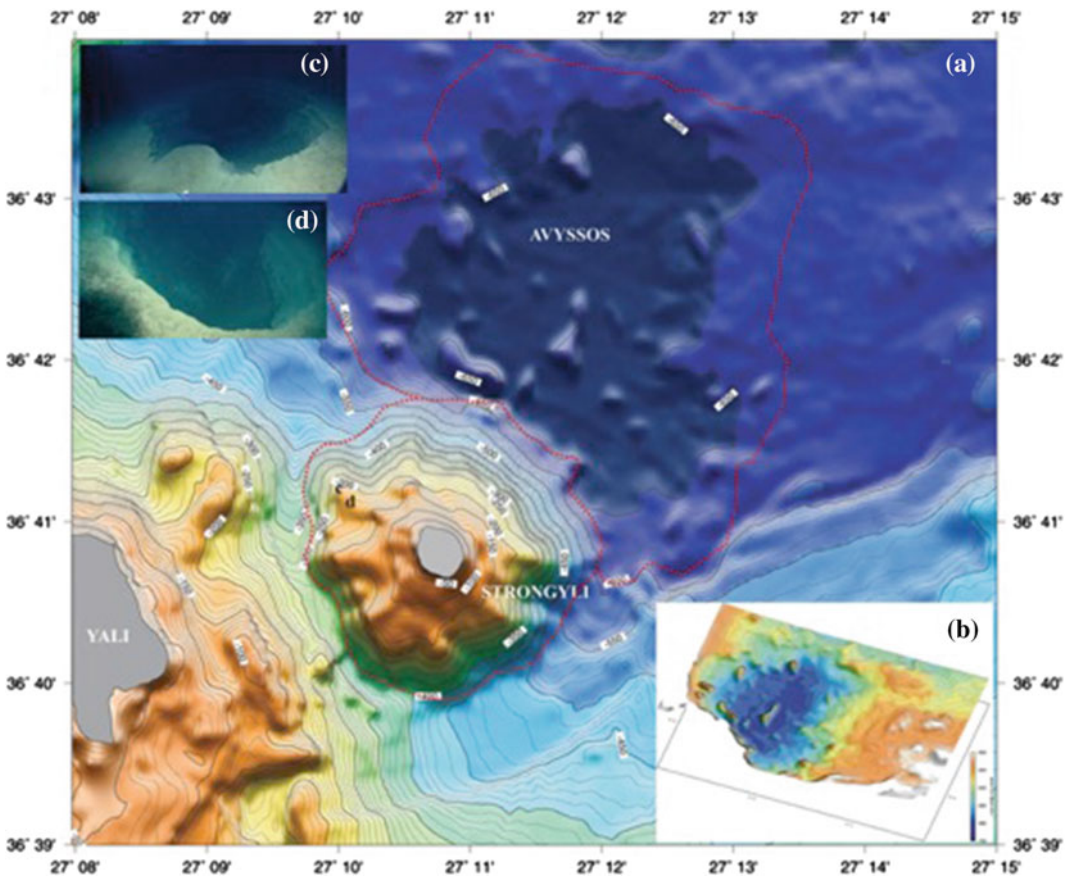


**Fig. 2.41** **a** Swath bathymetric map of Strongyli and Avyssos volcanoes using 10 m isobaths. *Red dotted lines* delineate the submarine volcanic outcrops; **b** 3-D map of the submarine caldera of “Abyssos” at depths between 600 and 680 m, using 2 m isobaths; **c** underwater crater observed during the dive of submersible THETIS in 2000 at 192 m depth, on the northwestern slopes of Strongyli

(point **c**); **d** underwater crater observed at depths ranging between 193 m (*at the top*) and 199 m (*at the bottom*) during 2010 exploration with ROV. The location (point **d**) is very close to the previous crater. A 6 m profile observed within the craters is made of layers of alternating pumice and ash. Nomikou 2004; Nomikou et al. (2013a, b)



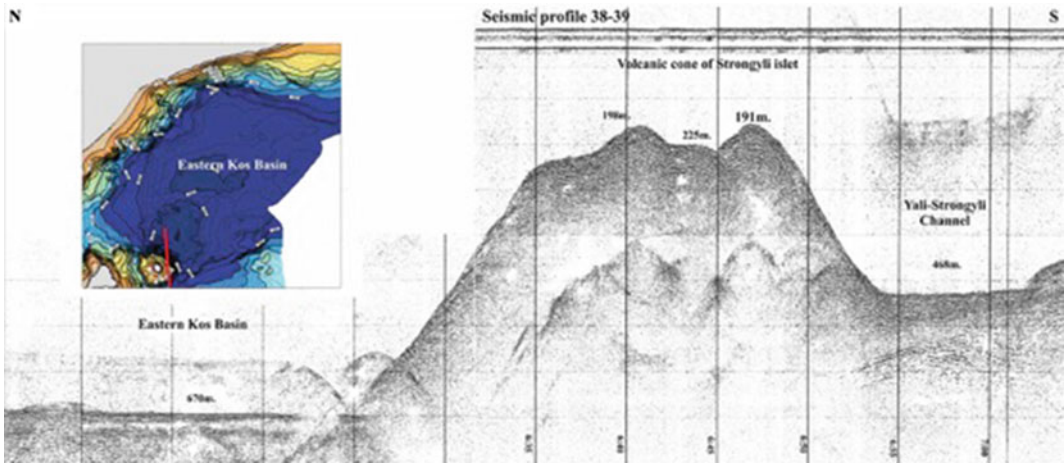


**Fig. 2.42** Representative air-gun profile from the area near Strongyli islet, showing characteristic hyperbolic reflectors corresponding to possibly submarine extinct

cinder cones (Nomikou 2004; Nomikou and Papanikolaou 2010b; Nomikou et al. 2013a, b)

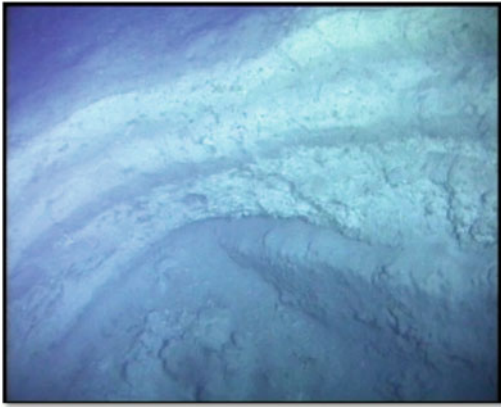


**Fig. 2.43** Part of the volcanic crater (8–10 diameter and 3,5–4 m height) at the Strongyli volcano at 240 m depth. Photos were taken by THETIS during 2000; (Nomikou 2004)

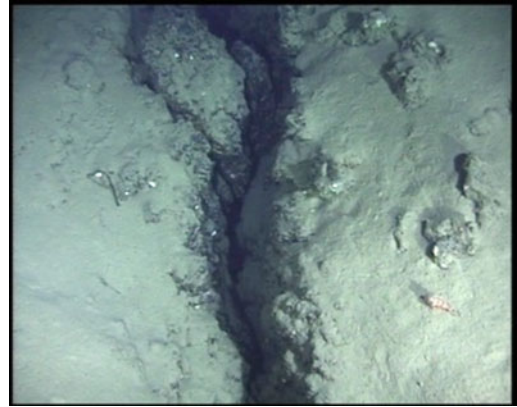


**Fig. 2.44** Open fracture across the slopes of the Strongyli volcanic cone at 390 m depth. Photos were taken by THETIS during 2000; (Nomikou 2004)

(Fig. 2.41c and 2.43) and several open fractures across the slope (2.44). Three transects of Strongyli's flanks were carried out using the ROV Hercules and Argus during the Nautilus cruise NA011 in 2010. These transects provide important information about the volcanic stratigraphy, underwater morphology, and structural features of the volcanic cone, such as fractures in different directions ranging mainly

between NE-SW to E-W. The walls of the fractures are made of heavily cemented bio-encrusted lava. Steep lava walls with evidence of shear are observed at the western part, covered by bio-encrusted sediments. Other outcrops at the northern slopes are covered by sediments with numerous small slide scars and most of the lava walls are heavily cemented and encrusted. New craters without any sign of hydrothermal activity,



aligned in the ENE-WSW direction, were discovered at depths around 190–200 m (Fig. 2.41d). The original morphology of the crater region is partially obliterated by thick pumice layers. An air-gun profile 38–39 (Fig. 2.42) across Strongyli islet shows the different level of the Avyssos abyssal plain (670 m) with respect to the Yali-Strongyli channel (470 m) on both sides of the Strongyli volcanic cone. An acoustically semi-transparent seismic unit with internal chaotic reflectors and diffraction hyperbolae appears either below the lower sequence or emerge above them in some areas between Nisyros and Yali and especially near the Strongyli islet (Nomikou and Papanikolaou 2010b; Nomikou et al. 2013a, b). These reflections reveal volcano-sedimentary deposits and volcanic domes.

### 2.3.3.6 Avyssos Crater

The largest underwater volcanic crater is located NE of Strongyli islet and was named “Avyssos Crater” because of its depth (600–700 m). This locality may correspond to a vent, from where the large volume of the “Kos Plateau Tuff” erupted. Since its discovery from swath mapping and air-gun seismic profiling, it has not been investigated until the Nautilus cruise NA011 in 2010 (Nomikou 2004a). The ROV Hercules was used to explore the slopes of the crater and the volcanic domes, which were identified on the base of detailed bathymetry obtained from multibeam data (Fig. 2.41a).

The “Avyssos Crater” dimensions are 3 km in the NW-SE direction and 4 km in the NE-SW direction. A hill of about 1 km length occurs at the center of Avyssos with relief of about 60–70 m, representing later intrusions of volcanic rocks within the almost planar base of the caldera (Fig. 2.41b). The stereographic diagram of Avyssos was constructed with 2 m isobaths to demonstrate the geometry of the volcanic structure. The peak of the central volcanic dome lies at 610 m depth, rising 66 m above the planar base of the caldera, which is at 676 m depth. The caldera rim lies at about 630 m depth forming a submarine circular cliff of 40–50 m topographic difference.

Seismic profiles had shown that there are only a few meters of sediment overlying the volcanic formations. The exploration of the Avyssos Crater showed that it is covered with fine-grained sediment, full of bioturbation holes and mounds without any evidence of hydrothermal activity. A few samples were collected from the intra-caldera volcanic hills, where the lavas are primarily cemented together with consolidated sediment bearing a black crust on the surface. Volcanic rocks were also sampled from the southern part of the crater.

### 2.3.3.7 The Volcanic Islets Pergousa and Pachia

The **Pergousa** volcanic edifice (Figs. 2.45 and 2.46) with altitudes between 65 and 83 m resembles in parts the pre-existence of a strato-volcano comprising weathered thick lava flows and domes covered by pumice deposits of the Kos Plateau Tuff. The latter contain bivalves and biogenic remains, indicating their submarine deposition. Several monolithic blocks and pyroclastic deposits are interpreted as witnesses of a nearby collapse structure. The predominantly porphyritic lavas are of andesitic to dacitic composition. Characteristic mineralogical features are abundant, partially resorbed amphibole, biotite, large plagioclase phenocrysts (up to 1 cm) and two pyroxenes and magnetite. The interstitial groundmass is made up of sparse glass and microliths of plagioclase, pyroxene and magnetite. No pumices from Nisyros and Yali have been found on both islands, Pergousa and Pachia, which points to a subaqueous position during the time of the young plinian eruptions on Nisyros and Yali and to a very recent uplift to expose the Kos ignimbrite deposits.

At the northwest coast of Pergousa islet, a gray, 1 m thick tuffite, rich in sponge needles, occurs. Marine terraces, similar to those on Yali Island, crop out along the shoreline of Pergousa. They are made up from calcite cement and contain abundant marine shells.

The volcanic edifice of **Pachia** islet (Figs. 2.45 and 2.47) is similar to that of Pergousa.

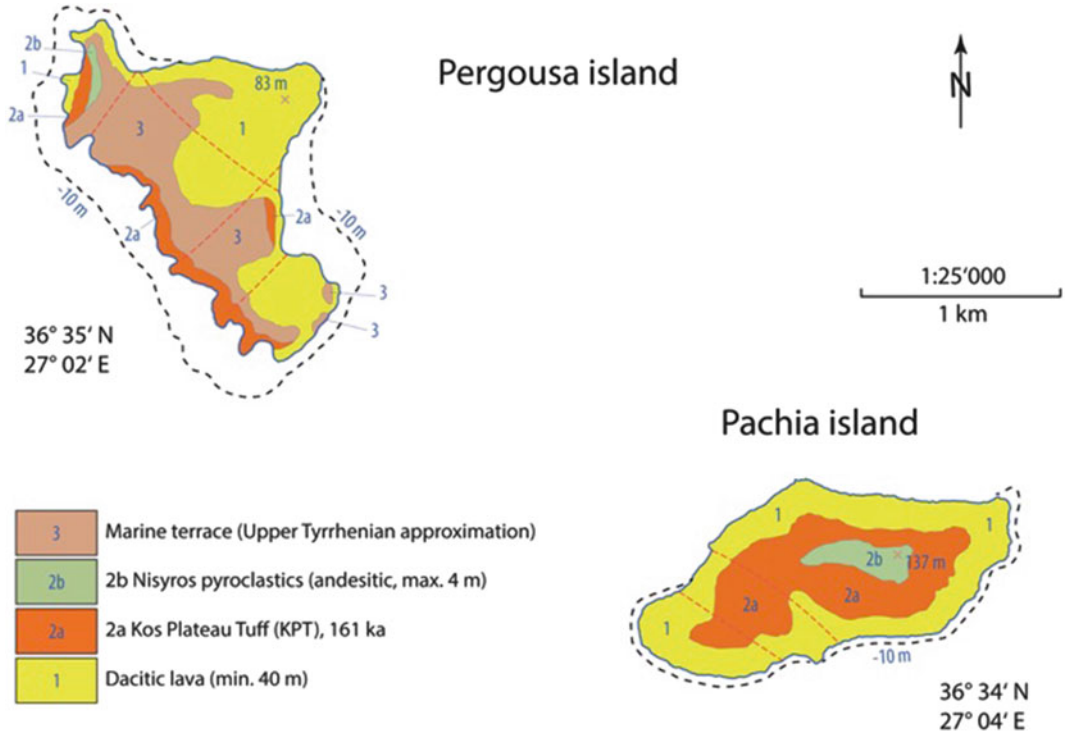


**Fig. 2.45** Geological maps of the islets of Pergousa and Pachia (geology redrawn and modified after “Nisyros sheet”; geological map of Greece 1:25,000, IGME (2003))

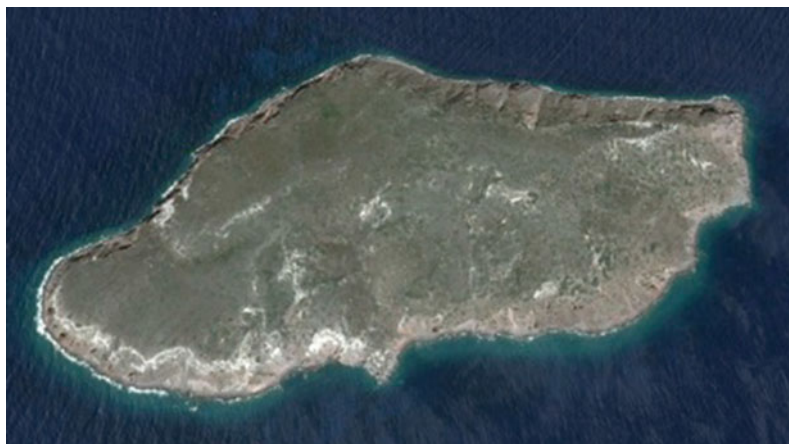
**Fig. 2.46** The volcanic islet of Pergousa (Google earth). The relief shows terraces covered with conglomerates. Gastropodes indicate a Pleistocene age. Image Google Earth



The basal dacitic lavas are overlain by two significant pumice sequences, (Fig. 2.45), which are correlated with the 161 ka Kos plateau eruption (Stadlbauer 1988; Keller et al. 1990; Vougioukalakis 1998). A lower, up to 3 m thick

sequence consisting of fine white ash with sub-parallel or cross-bedding layering, which contain sparse rounded white pumice lapilli and thin matrix-supported layers with reverse grading. These sedimentary structures are interpreted

**Fig. 2.47** The volcanic islet of Pachia. Image Google Earth



as depositions from surge pyroclastic density currents in sandwave phases.

The upper,  $\leq 5$  m thick sequence consists of a non-stratified lapilli tuff of white to gray pumice, which contains lithic blocks up to 1 m. One isolated lava block reaches a max. dimension of 6 m. Phenocrysts of sanidine, plagioclase, and biotite are present in the pumice. Equivalent deposits of the upper pumice sequence, up to 10 m thick, also occur in lower elevated parts of Pergousa islet.

The highest elevation part of Pachia islet is covered by a 1.5 m thick layer of gray coloured ash and fallout lapilli of andesitic composition containing a 10–15 cm thick with an interbedded paleosol, which may be correlated with an eruptive cycle during the period of the Nisyros composite stratovolcano (e.g. Nos. 18 and 19, Afionas tuff cone).

### 2.3.3.8 Kondelioussa Islet

Kondelioussa islet with an altitude of 100 m (Fig. 2.48a) forms a neotectonic horst consisting of Upper Jurassic (Malm) limestones (Fig. 2.45) is bordered by two marginal normal faults trending ENE-WSW, which have produced a subsidence of more than 1.3 km both towards the Western Nisyros Basin to the north and towards the Southern Nisyros Basin to the south (Nomikou and Papanikolaou 2010b). The above fault

throw is the minimum displacement, as estimated from the depth of the two basins (about 600 m for Western Nisyros and more than 1000 m for Southern Nisyros) and the thickness of the sediments below the sea bottom overlying the Alpine Mesozoic formations. The Kondelioussa limestones are detected all over the offshore continuation of the horst structure towards the west-southwest, below a post-Alpine sedimentary cover of about 100–150 m. The overall morphology of the horst offshore forms a platform with sediments tilted by 15–20° to the SW.

The analysis of the detailed swath bathymetric map and the seismic profiling has revealed several volcanic domes northeast of the islet and southwest of Nisyros (Nomikou 2004, Nomikou et al. 2013a). Submersible dive with THETIS of HCMR in 2000 at the northern flank of one of the volcanic domes discovered an underwater crater of several meters of diameter at 430 m depth (Fig. 2.48d), and thus confirmed the volcanic origin of the domes (Papanikolaou and Nomikou 2001). In 2010 on the E/V Nautilus, ROV Hercules explored the same area and found large fields of feather corals with elasmobranchs shark egg cases on them and patches of biogenic sediments with lots of sponges at 350 m depth. Other domes, northeast of Kondelioussa were explored in detail for the first time and their volcanic origin was confirmed but without any sign of hydrothermal

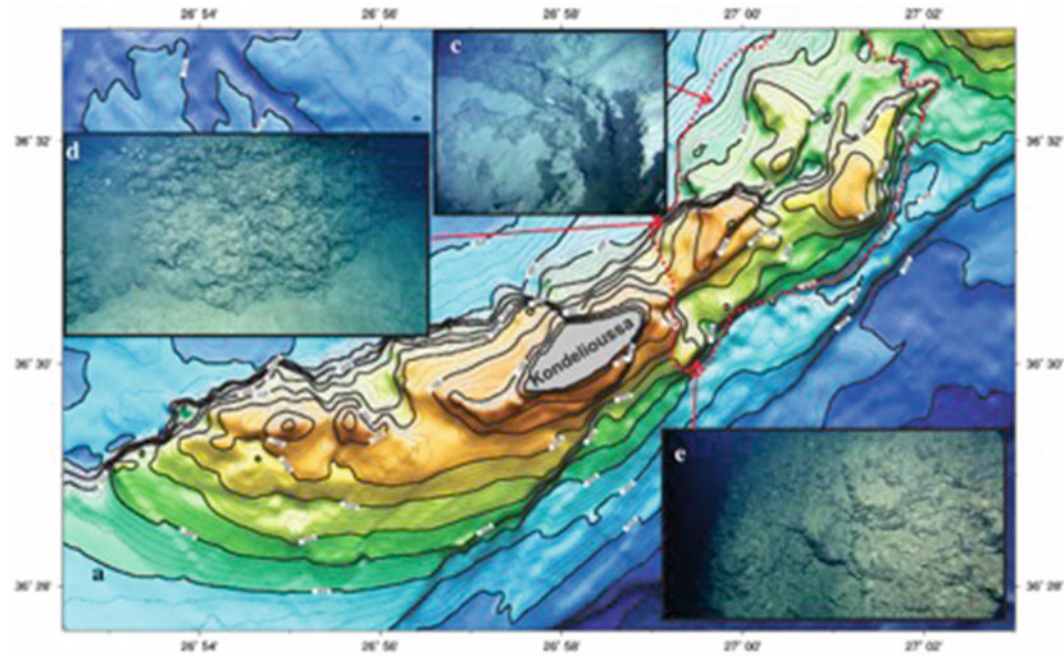


**Fig. 2.48** **a** Swath bathymetric map of Kondelioussa. The volcanic outcrops are delineated by *red dotted line*; **b** air gun single channel profile showing the volcanic domes east of Kondelioussa islet. The volcanic rocks form a horst structure separating the Western Nisyros Basin to the north (416 m) from the Southern Nisyros Basin to the south (522 m); **c-e** Photos were taken by THETIS during

2000 (crater at point **c**: and by ROV “Hercules” during 2010, showing steep vertical northern flank of the volcanic dome, NE of Kondelioussa at 330 m depth (point **d**: and large steep shear wall of lava covered by bio-encrusted sediments south of Kondelioussa (point **e**); Nomikou (2004), Nomikou et al. (2013a)

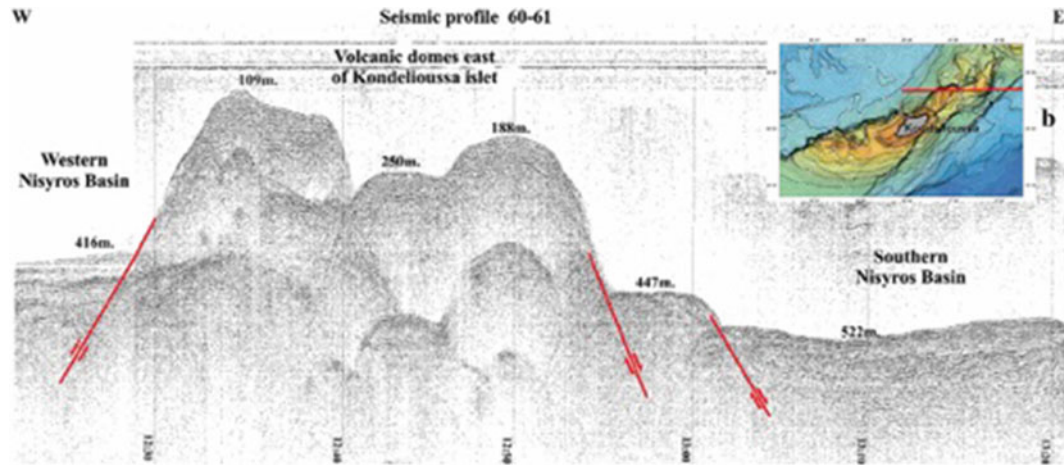


**Fig. 2.49** E-W seismic profile north of the island of Kondelioussa. Nomikou (2004), Nomikou et al. (2013a)



activity. The steep cliffs of the volcanic domes were sub vertical with many bio-encrustations (Fig. 2.48d, e). Lava samples were collected at the base of the lava outcrop with great difficulty.

ROV exploration of the northern vertical wall of the nearest volcanic dome NE of the islet indicated the location of the major NE-SW fault zone and revealed bio-encrusted solid lava layers (Fig. 2.48d, e) or fragmented pillow lavas covered by bio-encrustations at 263 m depth, as well as a reverse angle wall. Towards the west, columnar basalts were observed whereas at the SE margin of the islet steep rock surface with sub vertical lineations occurred along the tectonic boundary between the Mesozoic limestones towards the southwest and the recent volcanic rocks towards the northeast.

Several submarine volcanic domes have been found to the east of Kondeliousa islet (Fig. 2.49).

## References

- Allen SR (1998) Volcanology of the Kos Plateau Tuff, Greece: the product of an explosive eruption in an archipelago. PhD thesis, Monash University Australia
- Allen SR (2001) Reconstruction of a major caldera-forming eruption from pyroclastic deposit characteristics: Kos Plateau Tuff eastern Aegean Sea. *J Volcanol Geotherm Res* 105:141–162
- Allen SR, Cas RAF (1998a) Lateral variations within coarse co-ignimbrite lithic breccias of the Kos Plateau Tuff Greece. *Bull Volcanol* 59:356–377
- Allen SR, Cas RAF (1998b) Rhyolitic fallout and pyroclastic density current deposits from a phreato-plinian eruption in the eastern Aegean Sea Greece. *J Volcanol Geotherm Res* 86:219–251
- Allen SR, McPhie J (2000) Water-settling and resedimentation of submarine rhyolitic pumice at Yali eastern Aegean Greece. *J Volcanol Geotherm Res* 95:285–307
- Allen SR, Stadlbauer E, Keller J (1999) Stratigraphy of the Kos Plateau Tuff: product of a major quaternary explosive rhyolitic eruption in the eastern Aegean Greece. *Int J Earth Sci* 88:132–156
- Allen SR, Vougioukalakis GE, Schnyder C, Bachmann Dalabakis P (2009) Comments on: on magma fragmentation by conduit shear stress: evidence from the Kos Plateau Tuff Aegean Volcanic Arc by Palladino Simeï and Jyriakopoulos (JVGR 178 807-817). *J Volcanol Geotherm Res* 18:487–490
- Bachmann O (2010) The petrologic evolution and pre-eruptive conditions of the rhyolitic Kos Plateau Tuff (Aegean Arc). *Cent Eur J Geosci.* 2:270–305
- Bachmann O, Dungan MA, Lipman PW (2002) The fish Canyon magma body San Juan volcanic field Colorado: rejuvenation and eruption of an upper crustal batholith. *J Petrol* 43:1469–1503
- Bachmann O, Charlier BLA, Lowenstern JB (2007) Zircon crystallization and recycling in the magma chamber of the rhyolitic Kos Plateau Tuff (Aegean Arc) *Geology* 35(1):73–76
- Bachmann O, Schoene B, Schnyder C, Spikings R (2010)  $^{40}\text{Ar}/^{39}\text{Ar}$  and U/Pb dating of young rhyolites in the Kos-Nisyros volcanic complex, Eastern Aegean Arc (Greece): age discordance due to excess  $^{40}\text{Ar}$  in biotite. *Geochem Geophys Geosyst* 11:1–14
- Bardintzeff JM, Dalabakis P, Traineau M, Brousse R (1989) Recent explosive volcanic episodes on the island of Kos Greece: associated hydrothermal paragenesis and geothermal area of Volcania. *Terra Nova* 1:75–78
- Bellon H, Jarrige JJ (1979) Le magmatisme néogène et quaternaire de l'île de Kos (Grèce): données géologiques. *CR Acad Sci Paris Ser D* 228:1359–1362
- Böger H (1978) Sedimentary history and tectonic movements during the Late Neogene. In Closs H, Roeder D, Schmidt K (eds) *Alps Apennines Hellenides IUGS Rept*, vol 38, pp 506–509
- Böger H, Gersonde R, Willmann R (1974) Das Neogen im Osten der Insel Kos (Aegäis Dodekanes), Stratigraphie und Tektonik. *N Jb Geol Paläontol Abh* 145:129–152
- Bouvet de Maisonneuve C, Bachmann O, Burgisser A (2008) Characterization of juvenile pyroclasts from the Kos Plateau Tuff (Aegean Arc): insights into the eruptive dynamics of a large rhyolitic eruption. *Bull Volcanol*. doi:10.1007/s00445-008-0250-x
- Burri C, Tatar Y, Weibel M (1967) Zur Kenntnis der jungen Vulkanite der Halbinsel Bodrum (SW-Türkei). *Schweiz Miner Petro Mitt* 47:833–853
- Collins AS, Robertson AHF (1998) Process of late Cretaceous to late Miocene episodic thrust-sheet translation in the Lycian Taurides. *J Geol Soc Lond* 155:759–772
- Cooper KM, Kent AJR (2014) Rapid remobilization of magmatic crystals kept in cold storage. *Nature* 508:554
- Couch S, Sparks RSJ, Carroll MR (2001) Mineral disequilibrium in lavas explained by convective self-mixing in open magma chambers. *Nature* 411:1037–1039
- Dalabakis P (1986) Une des plus puissantes éruptions phréatomagmatiques dans la Méditerranée orientale: l'ignimbrite des Kos (Grèce). *Compt Rend l'Académie Sci Serie 2 Mécanique Physique Chimie Sciences de l'Univers. Sci Terre* 303:505–508
- Dalabakis P (1987) Le volcanisme récent de l'île de Kos. PhD Thesis, Univ Paris Sud Orsay Paris France 1987, 266 pp
- Dalabakis P, Vougioukalakis G (1993) The Kefalos tuff ring (W Kos): depositional mechanisms vent position and model of the evolution of the eruptive activity. *Bull Geol Soc Greece* 28(2):259–273 (in Greek with English abstract)

- Davis E, Gartzos E, Pavlopoulos A, Tsagalidis A (1993) Petrological and geochemical research of perlitites and rhyolites from Kefalos peninsula (island of Kos) and their quantitative evaluation (in Greek). In: Special volume in honour of Prof AG Panagos Athens A, pp 284–303
- Dietrich VJ, Oberhänsli R, Mercolli I, Gaitanakis P (1991) Geological Map of Greece Aegina Island (Saronic Gulf) 1:25,000 with expl. Stiftung Vulkaninstitut Immanuel Friedlaender Zürich Verlag Birkhäuser Basel und IGME (Athen)
- Di Paola GM (1974) Volcanology and petrology of Nisyros Island (Dodecanese Greece). *Bull Volcanol* 38:944–987
- Drakopoulos J, Delibasis N (1982) The focal mechanism of earthquakes in the major area of Greece for the period 1947–1981. Univ of Athens Seismological Laboratory No. 2
- Federman AN, Carey SN (1980) Electron microprobe correlation of tephra layers from Eastern Mediterranean abyssal sediments and the Island of Santorini. *Quatern Res* 13:160–171
- Francalanci L, Vougioukalakis GE, Perini G, Manetti P (2005) A west-east traverse along the magmatism of the South Aegean Volcanic Arc in the light of volcanological chemical and isotope data. In: M Fytikas, GE Vougioukalakis (eds) *The South Aegean active volcanic arc present knowledge and future perspectives developments in volcanology*. Elsevier, Amsterdam, pp 65–112
- Fytikas M, Guiliani O, Innocenti F, Marinelli G, Mazzuoli R (1976) Geochronological data on recent magmatism of the Aegean Sea. *Tectonophysics* 31:29–34
- Fytikas M, Innocenti F, Manetti P, Mazzuoli R, Peccerillo A, Villari L (1984) Tertiary to quaternary evolution of the volcanism in the Aegean region. In: Dixon JE, Robertson AHF (eds) *The geological evolution of the Eastern Mediterranean*, vol 17, pp 687–699 (Geol Soc London Spec Pub)
- Geotermica Italiana (1983) Nisyros 1 geothermal well PPC-EEC report, pp 1–106
- Geotermica Italiana (1984) Nisyros 2 geothermal well PPC-EEC report, pp 1–44
- GEOWARN (2003) GEOWARN geo-spatial warning system—synthesis report GEOWARN consortium Athens (Greece) and Zurich (Switzerland), 57 pp (<http://www.geowarn.org>)
- Hurni L, Dietrich VJ, Gaitanakis P (1995) Geological map of Greece Methana (Saronic Gulf) 1:25,000 with expl. Stiftung Vulkaninstitut Immanuel Friedlaender Zürich Verlag Birkhäuser Basel and IGME (Athen)
- IGME (2003) Nisyros sheet, geological map of Greece 1:25,000. Inst Geol Miner Explor, Athens Greece
- Innocenti R, Manetti P, Peccerillo A, Poli G (1981) South Aegean volcanic arc: geochemical variations and geotectonic implications. *Bull Volcanol* 44:377–391
- Jackson J (1993) Rates of active deformation in the Eastern Mediterranean. In: Boschi E et al (eds) *Recent evolution and seismicity of the Mediterranean region*. Kluwer Dordrecht, pp 53–64
- Jackson J (1994) Active tectonics of the Aegean region. *Ann Rev Earth Planet Sci* 22:239–271
- Jarigge X (1978) *Etudes neotectoniques dans l'arc volcanique egeen. Les lies de Kos, Santorini, Milos*. Thesis Univ Paris XI Paris France
- Keller J (1969) Origin of rhyolites by anatectic melting of granite and crustal rocks the example of rhyolitic pumice from the island of Kos (Aegean Sea). *Bull Volcanol* 33:942–959
- Keller J (1982) Mediterranean island Arcs. In: RS Thorpe (ed) *Andesites*. John Wiley, New York, pp 316–325
- Keller L, Rehren Th, Stadlbauer E (1990) Explosive volcanism in the Hellenic arc; a summary and review. In: Hardy DA, Keller J, Galanopoulos VP, Flemming NC, Druitt TH (eds) *Thera and the Aegean world III proceedings of the third international congress*, vol 2. The Thera Foundation, London, pp 13–26
- Kiss B, Harangi S, Ntaflos T, Mason PRD, Pál-Molnár E (2014) Amphibole perspective to unravel pre-eruptive processes and conditions in volcanic plumbing systems beneath intermediate arc volcanoes: a case study from Ciomadul volcano (SE Carpathians). *Contrib Mineral Petrol* 167:1–27
- La Ruffa G, Panichi C, Kavouridis T, Liberopoulou V, Leontiadis J, Caprai A (1999) Isotope and chemical assessment of geothermal potential of Kos island Greece. *Geothermics* 28:205–217
- Lagios E, Galanopoulos D, Hobbs BA, Dawes GJK (1998) Two dimensional magnetotelluric modelling of the Kos island geothermal region (Greece). *Tectonophysics* 287:157–172
- Le Pichon X (1982) Land-locked oceanic basins and continental collision: the Eastern Mediterranean as a case example. In: Hsü KJ (ed) *Mountain building processes*, vol 263, pp 201–211
- Le Pichon X, Angelier J (1979) The Hellenic arc and trench system: a key to the evolution of the Eastern Mediterranean. *Tectonophysics* 60:1–42
- Livanos I, Nomikou P, Papanikolaou D, Rousakis G (2013) Volcanic debris Avalanche at the SE submarine slopes of Nisyros Volcano Greece. *Geo Mar Lett* 33:419–431
- Makris J (1977) Geophysical investigations of the Hellenides. *Hamburger Geophysikalische Einzelschriften* 33:128 pp
- Makropoulos KC, Burton PW (1984) Greek tectonics and seismicity. *Tectonophysics* 106:275–304
- Makropoulos K, Drakopoulos J, Latoussakis J (1989) A revised earthquake catalogue for Greece since 1900. Publ No 2. *Geophys J Int* 98:391–394
- McKenzie DP (1972) Active tectonics of the Mediterranean Region. *Geophys J R Astron Soc* 30:109–185
- Molloy C, Shane P, Nairn I (2008) Pre-eruption thermal rejuvenation and stirring of a partly crystalline rhyolite pluton revealed by the Earthquake Flat Pyroclastics deposits, New Zealand. *J Geol Soc London* 165:435–447

- Müeller St, Kahle HG (1993) Crustmantle evolution, structure and dynamics of the Mediterranean-Alpine region. In: Smith, Turcotte (eds) Contributions of Space Geodesy to Geodynamics: crustal Dynamics, American Geophysical Union (AGU), Geodynamics Series, Washington D.C. 23:249–298
- Murphy MD, Sparks RSJ, Barclay J, Carroll MR, Brewer TS (2000) Remobilization of andesitic magma by intrusion of mafic magma at the Soufrie're Hills Volcano Montserrat West Indies. *J Petrol* 41:21–42
- Nakamura M (1995) Continuous mixing of crystal mush and replenished magmain the ongoing Unzen eruption. *Geology* 23:807–810
- Nomikou P (2004) Geodynamics of Dodecanese islands: Kos and Nisyros volcanic field. PhD thesis, Department of Geology University of Athens 467 pp
- Nomikou P, Papanikolaou D (2000) Active geodynamics at Nisyros the eastern edge of the Aegean volcanic arc: emphasis on submarine surveys proceedings of the 3rd international conference geology East Mediterranean Sept 1998, pp 97–103
- Nomikou P, Papanikolaou D (2010a) A comparative morphological study of the Kos-Nisyros-Tilos volcanosedimentary basins. *Bull Geol Soc Greece* 43:464–474
- Nomikou P, Papanikolaou D (2010b) The morphotectonic structure of Kos-Nisyros-Tilos volcanic area based on onshore and offshore data XIX Congress of the Carpathian-Balkan geological association Thessaloniki Greece 23–26 Sept 2010. *Proc Spec* 99:557–564
- Nomikou P, Papanikolaou D (2011) Extension of active fault zones on Nisyros Volcano across the Yali-Nisyros Channel based on onshore and offshore data. *Mar Geophys Res* 32:181–192
- Nomikou P, Papanikolaou D, Alexandri S, Ballas D (2004) New insights on the Kos–Nisyros volcanic field from the morphotectonic analysis of the swath bathymetric map. *Rapp Comm Int Mer Medit* 37:60
- Nomikou P, Tibaldi A, Pasquare F, Papanikolaou D, (2009) Submarine Morphological analysis based on multibeam data of a huge collapse at the SE flank of Nisyros volcano International Conference on Seafloor Mapping for Geohazard Assessment 11–13 May Ischia Italy. *Rend Soc Geol It* 7:177–179
- Nomikou P, Bell KLC, Vougioukalakis G, Livanos I, Martin Fero J (2011) In: Bell KLC, Fuller SA (eds) Exploring the Nisyros volcanic field: p 27. In: New frontiers in ocean exploration: the E/V nautilus 2010 field season. *Oceanography*, vol 24(1) supplement
- Nomikou P, Papanikolaou D, Alexandri M, Sakellariou D, Rousakis G (2013a) Submarine volcanoes along the Aegean volcanic arc. *Tectonophysics* 507–508:123–146
- Nomikou P, Croff Bell K, Papanikolaou D, Livanos I, Fero Martin J (2013b) Exploring the submarine flanks of Yali and Strongyli volcanic islets at the eastern edge of the Aegean Volcanic Arc. *Zeitschrift Geomorphologie* 57(Suppl 3):125–137
- Nomikou P, Papanikolaou D, Tibaldi A, Carey S, Livanos I, Bell KLC, Pasquare FA, Rousakis G (2013c) The detection of volcanic debris Avalanches along the Hellenic volcanic arc through marine geophysical techniques. In: Submarine mass movements and their consequences, 5th vol, pp 337–349 (Chapter 30)
- Pallister JS, Hoblitt RP, Reyes AG (1992) A basalt trigger for the 1991 eruptions of Pinatubo volcano? *Nature* 356:426–428
- Papadopoulos GA (1984) Seismic properties in the eastern part of the South Aegean Volcanic Arc. *Bull Volcanol* 47:143–152
- Papadopoulos GA, Kondopoulou DP, Levendakis GA, Pavlides SD (1986) Seismotectonics of the Aegean region. *Tectonophysics* 124:67–84
- Papanikolaou DJ (1993) Geotectonic evolution of the Aegean. *Bull Geol Soc Greece* 18:33–48
- Papanikolaou DJ, Lekkas E (1990) Miocene tectonism in Kos Dodekanese islands IESCA Izmir 1990 abstracts, pp 179–180
- Papanikolaou D, Nomikou P (1998) The Palaeozoic of Kos: “A low grade metamorphic unit of the basement of the External Hellenides Terrane” *Spec Publ Geol Soc Greece* 3, IGCP Project 276 Newsletter 6:155–166
- Papanikolaou D, Nomikou P (2001) Tectonic structure and volcanic centres at the eastern edge of the Aegean volcanic arc around Nisyros island. *Bull Geol Soc Greece* 34:289–296
- Papanikolaou DJ, Lekkas EL, Sakellariou DT (1991) Geological structure and evolution of Nisyros volcano. *Bull Geol Soc Greece* 25:405–419
- Pe G, Piper DJW (1972) Volcanism at subduction zones. The Aegean area. *Bull Geol Soc Greece* 9:113–144
- Pe-Piper G, Piper DJW (2002) The igneous rocks of Greece. The anatomy of an orogen. *Gebr Bornträger*, Berlin Stuttgart 573 pp
- Pe-Piper G, Piper DJW (2005) The South Aegean active volcanic arc: relationships between magmatism and tectonics. In: Fytikas M, Vougioukalakis GE (eds) The South Aegean active volcanic arc present knowledge and future perspectives developments in volcanology. Elsevier, Amsterdam, pp 113–134
- Pe-Piper G, Piper DJW, Kotopouli CN, Panagos AG (1994) Neogene volcanoes of Chios Greece: relative importance of subduction and back-arc extension. In: Smellie JL (ed) Volcanism associated with extension at consuming plate margins. *Geol Soc Lond Spec Publ* 81:213–232
- Piper DJW, Pe-Piper G, Lefort D (2010) Precursory activity of the 161 ka Kos Plateau Tuff eruption Aegean Sea (Greece). *Bull Volcanol*. doi:10.1007/s00445-010-0349-8
- Robertson AHF, Dixon JE (1984) Introduction aspects of the geological evolution of the eastern Mediterranean In: Dixon J, Robertson AHF (eds) The geological evolution of the eastern Mediterranean. *Geol Soc Lond Spec Publ* 17:1–74

- Smith AG (1971) Alpine deformation and the oceanic areas of the Tethys Mediterranean and Atlantic. *Geol Soc Am Bull* 82:2039–2070
- Smith PE, Evensen NM, York D (2000) Under the volcano: a new dimension in Ar-Ar dating of volcanic ash. *Geophys Res Lett* 27:585–588
- Smith PE, York D, Chen Y, Evensen NM (1996) Single crystal  $^{40}\text{Ar}/^{39}\text{Ar}$  dating of a late quaternary paroxysm on Kos Greece, concordance of terrestrial and marine ages. *Geophys Res Lett* 23:3047–3050
- Stadlbauer E (1988) Vulkanologisch-geochemische Analyse eines jungen Ignimbrits: der Kos-Plateau-Tuff (Südost-Ägäis). PhD thesis Albert-Ludwigs-Universität Freiburg im Breisgau, 184 pp
- Tibaldi A, Pasquarè FA, Papanikolaou D, Nomikou P (2008a) Discovery of a huge sector collapse at the Nisyros volcano Greece by on-land and offshore geological-structural data. *J Volcanol Geotherm Res* 177:485–499
- Tibaldi A, Pasquarè FA, Papanikolaou D, Nomikou P (2008b) Tectonics of Nisyros Island Greece by field and offshore data and analogue modeling. *J Struct Geol* 30:1489–1506
- Triantaphyllis M (1994) Geological map of Greece western Kos, sheet (Kefalos) 1:50,000 inst geology mineral exploration (IGME) Athens Greece
- Triantaphyllis M, Mavrides A (1998) Geological map of Greece Eastern Kos, sheet (Kos) 1:50,000 inst geology mineral exploration (IGME) Athens Greece
- Volentik A, Vanderkluysen L, Principe C, Hunziker JC (2005) Stratigraphy of Nisyros Volcano (Greece). In: Hunziker JC, Marini L (eds) The petrology and geochemistry of lavas and tephra of Nisyros Volcano (Greece). *Mém Géologie (Lausanne)* 44:26–66
- Vougioukalakis GE (1998) Blue volcanoes: Nisyros Nisyros. Regional Council Mandraki 78pp
- Wagner GJ, Storzer D, Keller J (1976) Spaltspurendatierungen quartärer Gesteinsgläser aus dem Mittelmeerraum. *N Jb Miner Mh* 2:84–94



Nisyros Volcano

The Kos - Yali - Nisyros Volcanic Field

Dietrich, V.J.; Lagios, E. (Eds.)

2018, XII, 339 p. 472 illus., 449 illus. in color.,

Hardcover

ISBN: 978-3-319-55458-7